MAUSAM, **70**, 4 (October 2019), 667-690

551.515.2

An inner-core analysis of the axisymmetric and asymmetric intensification of tropical cyclones: Influence of shear

SUNDARARAMAN G. GOPALAKRISHNAN, KRISHNA K. OSURI*,

FRANK D. MARKS and U. C. MOHANTY**

Hurricane Research Division, *AOML*, *NOAA Miami*, *Florida*, *33149*, *USA*

**Department of Earth* and *Atmospheric Sciences*, *NIT Rourkela*, *Odisha*, *769 008*, *India*

***School of Earth Ocean* and *Climate Sciences*, *IIT Bhubaneswar*, *Odisha*, *752 050*, *India*

e mail : sundararaman.g.gopalakrishnan@noaa.gov

सार - तूफान मौसम अनुसंधान और पूर्वानुमान (HWRF) मॉडलिंग प्रणाली को आधार के रूप में उपयोग करके अत्याधुनिक समय में तूफान की तीव्रता का पूर्वानुमान प्रदान किया जाता है। उष्णकटिबंधीय चक्रवातों (टीसीएस) की तीव्रता के लिए मौजूदा अक्षीय सिद्धांत की संक्षिप्त समीक्षा भी प्रदान की गई है। एक आदर्श स्थिति और दूसरा महा चक्रवात फिलिन (2013) की अक्षसममिति, तीव्र तीव्रता (आरआई) प्रणाली को समझने के लिए तूफान मौसम अनुसंधान और पूर्वानुमान (HWRF) से प्राप्त दो क्लाउड-रिज़ॉल्यूशन सिमुलेशन उपयोग किया जाता है। हालांकि, उष्णकटिबंधीय चक्रवात विरले ही कभी अक्षसममित होते हैं। एक उष्णकटिबंधीय चक्रवात के आंतरिक कोर में असममित संरचना दोनों आंतरिक गतिशीलता और वायुमंडलीय कारक जैसे - अपरूपण और नमी के कारण बाहरी बल दोनों के द्वारा उत्पन्न हो सकती है। हम उष्णकटिबंधीय चक्रवातों के तीव्र तीव्रीकरण पर अपरूपण प्रेरित अक्षसममित की भूमिका को समझने के लिए अटलांटिक तूफान अर्ल (2010) से चलाए जाने वाले एक पूर्वव्यापी एचडब्ल्यूआरएफ का उपयोग करते हैं। इस संबंध में हम निम्नलिखित प्रश्नों को हल करना चाहते हैं : *उष्णकटिबंधीय चक्रवात किस तरह से एक क्षीण वातावरण में तेजी के साथ तीव्र हो जाता है? उष्णकटिबंधीय चक्रवात की तीव्रता पर भंवर प्रवाह की भूमिका क्या है? क्या आरआई के दौर से गुजरने वाले अपरूपित तूफानों के लिए उष्णकटिबंधीय चक्रवात की तीव्रता से स्वीकृत सैद्धांतिक रूपरेखा अभी भी मान्य है?*

हमारे निष्कर्ष और अन्य समानांतर शोध बताते हैं कि अपरूपण तूफानों में उष्णकटिबंधीय चक्रवात की तीव्रता में परिवर्तन को नियंत्रित करने में भंवर की रेडियल वोरटिसिटी फ्लक्स महत्वपूर्ण भूमिका निभाती है। अर्ल के मामले में, लगातार पर्यावरणीय अपरूपण और सममित संवहन की कमी के बावजूद, मेसोस्केल संवहन परिसरों द्वारा बनाई गई ऊपरी ट्रोपोस्फीयर के बीच में एक सकारात्मक भंवर वर्टिसिटी प्रवाह का उष्णकटिबंधीय चक्रवात के स्पिन-अप प्रक्रिया को तेज करने में गहरा प्रभाव रहा। तीव्र तीव्रीकरण तब तक नहीं होता है जब तक कि लगातार संवहनी विस्फोट नहीं होता है और सतह के केंद्र से लगभग 50 किमी की दूरी पर नीचे-बाएँ चतुष्कोण में संकुचित वर्टिसिटी केंद्रित होती है, इसके बाद इन परिसरों का उत्थान तेज गति से होता है। जब संवहनी फटने के बाद बाएं चतुर्थांश तक पहुंचते हैं, तो भंवर रेडियल वर्टिसिटी फ्लक्स का लगभग सममित पैटर्न केंद्र को घेरता है, जो यह दर्शाता है कि वर्टिसिटी विसंगतियां एक मजबूत माध्यिका तंत्र बनाने के लिए विलीन हो गई हैं जिसमें ऊपरी और निचले स्तर के परिसंचरण बेहतर रूप से संरेखित होते हैं। यह प्रक्रिया एक विशिष्ट भंवर से अलग है। एक विशिष्ट भंवर एक अपरूपण-मुक्त वातावरण में तेज होता है, जहां व्यक्तिगत वर्टिकल हॉट प्लम मिल जाते है और लघु स्तरीय भ्रमिलता का परिवेशी विस्तार छोटे पैमाने की विसंगति मानी जाती है और इन प्लमों के कई विलयन भ्रमिलता से पूर्ण वातावरण में एकल भंवर की ओर ले जाते हैं। विशिष्ट मामले में, भंवर का प्रमुख स्पिन-अप उष्णकटिबंधीय चक्रवात सीमा परत और अक्षीय गोलक क्षेत्र में होता है, जबकि अर्ल के मामले में स्पिन-अप तीव्र तीव्रीकरण (आरआई) के शुरुआती चरणों के दौरान शीर्ष-नीचे प्रतीत होता है। फिर भी, अर्ल के प्रारंभिक तीव्र तीव्रीकरण (आरआई) चरण के बाद सीमा परत में मजबूत स्पिन-अप के प्रमाण देखे गए हैं। यद्यपि वास्तविक उष्णकटिबंधीय चक्रवात तीव्रता की समस्या को समझने के लिए एक पूरी तरह से त्रि-आयामी मॉडल की आवश्यकता होती है, जब अक्षीय रूप से औसतन ढांचे से देखा जाता है, तीव्रीकरण का मूल अक्षीय सिद्धांत अभी भी सभी स्थितियों के लिए मान्य है।

ABSTRACT. The state-of-the-art in intensity forecasting is provided using the Hurricane Weather Research and Forecasting (HWRF) modeling system as the basis. A brief review of existing axisymmetric theory for the intensification of tropical cyclones (TCs) is also provided. Two cloud-resolving simulations from HWRF, one from an idealized case and another from a retrospective forecast of Super Cyclone Phalin (2013), are used to understand the axisymmetric, rapid

intensification (RI) process. However, TCs are rarely axisymmetric. The asymmetric structure in the inner core of a TC may be generated by both internal dynamics and external forcing due to environmental factors such as shear and moisture. We use a retrospective HWRF run from Atlantic Hurricane Earl (2010) to understand the role of shear-induced asymmetries on the RI of TCs. We seek to address the following questions: *How do TCs rapidly intensify in a sheared environment? What is the role of eddy fluxes on TC intensification? Is the well-accepted theoretical framework of TC intensification still valid for sheared storms undergoing RI?*

Our findings show that eddy radial vorticity fluxes play a significant role in controlling TC intensity changes in sheared storms. In the case of Earl, despite persistent environmental shear and a lack of symmetric convection, a positive eddy vorticity flux in the middle to upper troposphere created by mesoscale convective complexes had a profound influence in accelerating the TC spin-up process. RI does not occur until persistent convective bursts and the collocated vertical vorticity are concentrated in the downshear-left quadrant about 50 km from the surface center, followed by the propagation of these complexes in an upshear direction. When convective bursts reach the upshear-left quadrant, a nearly symmetric pattern of eddy radial vorticity flux surrounds the center, indicating vorticity anomalies have merged to create a stronger mean vortex wherein the upper and lower level circulations are better aligned. This process is different from that of an idealized vortex. An idealized vortex intensifies in a shear-free environment where individual vortical hot plumes converge and stretch ambient low-level vorticity into a small-scale anomaly and multiple mergers of these plumes lead to a single stronger vortex in a vorticity rich environment. In the idealized case, the major spin-up of the vortex occurs in the TC boundary layer and eyewall region, while spin-up in the case of Earl appears to be top-down during the early stages of RI. Nevertheless, evidence of stronger spin-up is observed in the boundary layer after Earl's initial RI phase. Although a fully three-dimensional model is required to understand the real TC intensification problem, when viewed from an axially-averaged framework, the basic axisymmetric theory of intensification is still valid for all cases.

Key words – Tropical cyclones, Vorticity.

1. Introduction

Predicting intensity changes, in general and rapid intensity changes, in particular, in tropical cyclones (TCs) is a complex and challenging multiscale problem. Apart from the well-documented impacts of the upper ocean (e.g., Byers, 1944; Black, 1983; Shay *et al.*, 2000; Halliwell *et al.*, 2015), environmental factors such as wind shear (e.g., Gray, 1968; Merrill, 1988; DeMaria and Kaplan, 1994; Chen and Gopalakrishnan, 2015; Leighton *et al.*, 2018), moisture in the low to middle troposphere (e.g., Gray 1968) and inner-core processes ranging from convective to mesoscale (e.g., Schubert and Hack, 1982; Hack and Schubert, 1982; Willoughby *et al.*, 1982; Kossin and Schubert, 2001; Eastin *et al.*, 2005a,b; Chen and Gopalakrishnan, 2015) are all known to influence intensity changes. These factors interact in a nonlinear fashion, making the TC intensification problem a complex forecast issue.

Early guidance and warnings could save lives and reduce property damages due to severe weather. In 2009 the National Oceanic and Atmospheric Administration (NOAA) established the 10-year Hurricane Forecast Improvement Program (HFIP) to improve the accuracy and reliability of hurricane forecasts; to extend lead time for hurricane forecasts with increased certainty; and to increase confidence in hurricane forecasts. The specific goals of HFIP included: reducing intensity errors by 20% in 5 years and by 50% in 10 years; increasing the probability of detection, especially for Rapid Intensification (RI)[1] and rapid weakening in TC events; and decreasing false alarms for RI change. The high-resolution Hurricane Weather Research and Forecasting (HWRF) model was jointly developed by NOAA's National Weather Service/ National Centers for Environmental Prediction (NWS/NCEP) and the Hurricane Research Division (HRD) of the Atlantic Oceanographic and Meteorological Laboratory (AOML) in response to HFIP (Gopalakrishnan *et al.*, 2011, 2012, 2013; Bao *et al.*, 2012; Tallapragada *et al.*, 2014; Atlas *et al.*, 2015). The modeling system is now paving the way in removing the initial roadblocks associated with predicting intensity changes, the dynamical prediction of which was nearly non-existent before 2009 (Gopalakrishnan *et al.*, 2019). Since 2011, HWRF intensity predictions for the Atlantic basin have improved by about 40-60% (Gopalakrishnan *et al.*, 2019). HWRF has been run operationally in all global basins since 2014 and used by forecasters for reliable (track and) intensity guidance (Tallapragada *et al.*, 2015a,b). For instance, HWRF is the operational TC forecasting system used by the India Meteorological Department (IMD) for tracking TCs over the Indian Seas (Mohanty *et al.*, 2015). Figs. 1(a-d) shows an HWRF forecast from one cycle of a forecast for rapidly intensifying TC Phailin (2013) and rapidly weakening TC Lehar (2013).

Significant improvements to the HWRF system are attributed to a number of major changes since 2012. These improvements include a new, higher-resolution TC following moving nest capable of better resolving eyewall convection and scale interactions between the nest and regional domain (Gopalakrishnan *et al.*, 2011, 2012), an inner core data assimilation technique, improved planetary boundary layer (PBL) and turbulence physics (Gopalakrishnan *et al.*, 2013), an improved nest

[1] RI is defined as an increase in 10-m maximum sustained winds of at least 30 knots in a 24-hour period. This goal for HFIP also applies to rapid weakening, *i.e.*, a decrease of 25 knots in 24 hours.

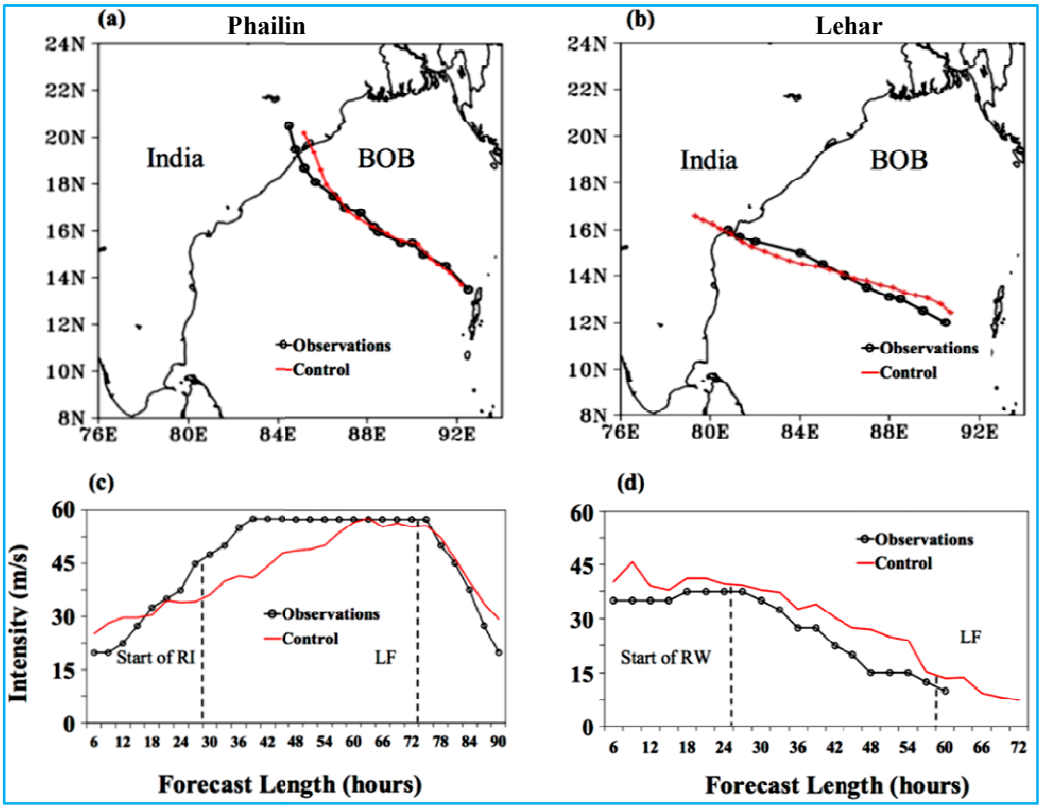

Figs. 1(a-d). An example of rapidly intensifying and weakening HWRF forecasts: (a) TC Phailin initialized at 1200 UTC, 9 October 2013 and (b) TC Lehar initialized at 0000 UTC, 26 November 2013. (c & d) are the same as (a & b) but for intensity where the start of RI/RW and the landfall points are indicated with dashed lines. BOB: Bay of Bengal

motion algorithm (Zhang *et al.*, 2016) and, above all, yearly upgrades, systematic testing and evaluation based not only on single simulations and idealized case studies but also on several seasons of testing (Tallapragada *et al.*, 2015a,b).

Yet, predicting RI events still poses major forecasting challenges. Fig. 2 demonstrates the difficulties associated with RI forecasts, for instance, the case of Hurricane Harvey (2017) in the Atlantic basin. While some of the later cycles from HWRF predicted RI in Harvey more accurately, a few other cycles missed the event. Cycle-to-cycle and TC-to-TC variability in RI predictions with numerical models is, in general, not uncommon.

Much of the lack of improvement in RI forecast skill is rooted in our lack of understanding of how and when RI occurs in different environmental conditions. It is also rooted in the historic inability of dynamical models to accurately predict convection in the TC core, as well as large scale environmental factors such as shear (and moisture) that can influence RI events (Chen and Gopalakrishnan, 2015; Leighton *et al.*, 2018). A number of mechanisms have been proposed to explain the negative influence of shear on the evolution of TCs. These mechanisms include tilting of the vortex (e.g., DeMaria, 1996; Balachandran *et al.*, 2019), "ventilation" of the warm core in the upper levels (Gray, 1968; Frank and Ritchie, 2001), mid-level ventilation (Tang and Emanuel, 2010, 2012) and the reduction of moist entropy by shear-induced persistent downdrafts that flush relatively cool, dry air into a TC's inflow layer (Riemer *et al.*, 2010). All of these mechanisms have been shown to impede TCs from reaching their potential intensity. At the same time, recent findings have shown that tropical depressions and weak storms can grow and rapidly intensify in a sheared environment (Molinari *et al.*, 2006; Reasor *et al.*, 2009; Molinari and Vollaro, 2010; Chen and Gopalakrishnan, 2015; Fischer *et al.*, 2017; Leighton *et al.*, 2018; Chen *et al.*, 2018). For example, Atlantic Hurricane Earl (2010) intensified in an environment of nearly constant shear of about 5 ms^{-1} and, more recently, Atlantic Hurricane Michael (2018) intensified in an environment where shear was stronger than 10-15 m s^{-1}. *How do TCs rapidly intensify in a sheared environment?*

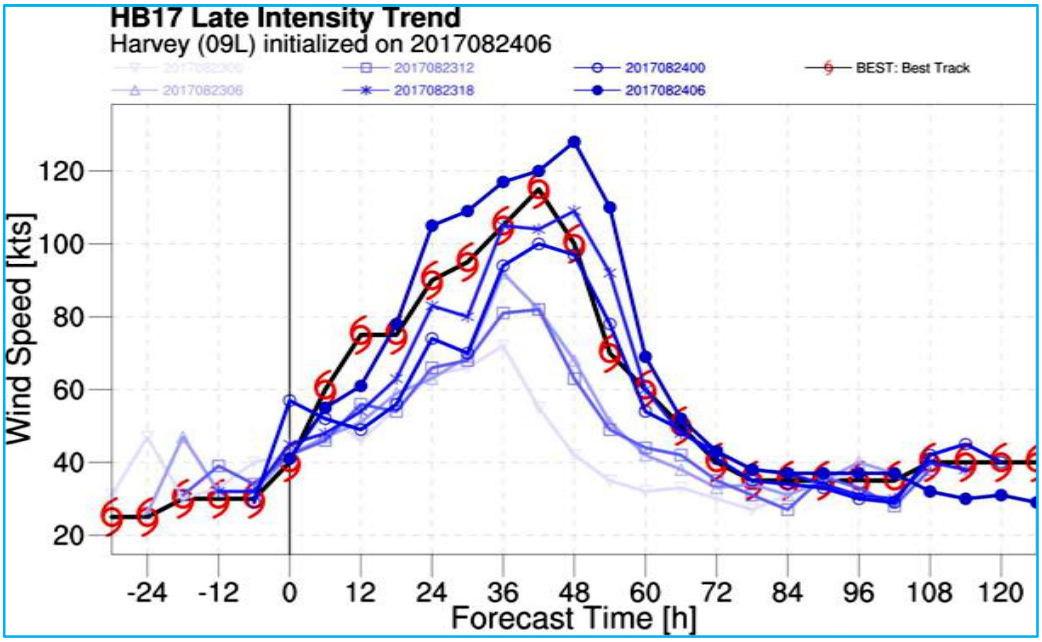

Fig. 2. Example of cycle-to-cycle variability in RI predictions. Six cycles of Atlantic Hurricane Harvey (2017) forecasts using an experimental version of HWRF

Kaplan and DeMaria (2003) found that about 30% of 159 episodes of RI reported in Atlantic hurricanes between 1989-2000 experienced a deep layer of shear of about 4-6 ms^{-1}. Consequently, shear-vortex interaction in TCs is also an important forecasting problem.

Past studies, starting with the pioneering theoretical work of Riehl (1954), Ooyama (1969, 1982) and Emanuel (1986) supported with inner-core observations (Willoughby, 1979, 1990a, 1990b), have all led to a well-accepted understanding of the axisymmetric inner-core structure and intensification of a TC[2]. Idealized simulations have shown that after an initial period of gestation where the spin-up of a modeled TC vortex takes place, a period of RI is observed that continues for up to 12-36 hours (e.g., Ooyama, 1969; Nguyen *et al.*, 2011; Gopalakrishnan *et al.*, 2011, 2013; Montgomery and Smith, 2014). During this time, the central pressure drops and the maximum 10 m wind speed increases rapidly until a quasi-steady state near a potential intensity limit is reached. However, environmental shear, which is not uncommon in a real environment, has a significant effect on the inner-core structure and intensification of a TC. Shear creates asymmetries in convection. In this case, *is the well-accepted theoretical framework of TC intensification still valid for sheared storms undergoing RI?*

We address this question by using output data from three simulations generated from the triple-nested (27:9:3 km), cloud-resolving version of the operational HWRF system. HWRF can be run in both idealized and operational modes[3] (Gopalakrishnan *et al.*, 2011, 2012, 2013; Bao *et al.*, 2012; Tallapragada *et al.*, 2014; Atlas *et al.*, 2015). The three simulations we used are from (*i*) an idealized case reported in Gopalakrishnan *et al.* (2013; GK2013, henceforth), (*ii*) the 1200 UTC cycle of 9 October 2013 for Super Cyclone Phailin (Osuri *et al.*, 2017; O2017, henceforth) and (*iii*) the 1800 UTC cycle of 26 August 2010 for the retrospective forecast of Atlantic Hurricane Earl (Chen and Gopalakrishnan, 2015; CG2015, henceforth). For analysis, the outputs from the HWRF model were interpolated from the original rotated latitude-longitude vertical hybrid coordinate system to the cylindrical polar height coordinate system.

Details of the Idealized (GK2013) simulation: The first simulation used in this work was an idealized HWRF run described in GK2013 (for alpha = 0.25 case in that work). For this experiment, the nonlinear balance equation in the pressure-based sigma coordinate system described in Wang (1995) was solved within the rotated latitude-longitude E-grid of the HWRF framework, where the

[2] Readers are also referred to articles by Montgomery a Smith (2014) and Smith and Montgomery (2015) for an excellent review on the axisymmetric TC vortex spin-up problem.

[3] After every yearly upgrade, the HWRF system is available in a public repository maintained by the Developmental Testbed Center, University Corporation for Atmospheric Research, Boulder, Colorado, USA. Readers are kindly recommended to refer to the *HWRF User's Guide* for additional details about the system (https://dtcenter.org/HurrWRF/users/docs/index.php).

mass field was obtained from the wind field. The calculations were performed on an *f*-plane centered at 15° N. In this idealized experiment, an axisymmetric vortex was initialized with a wind maximum of 20 ms^{-1} at a radius of ~90 km embedded in a uniform easterly flow of 4 ms^{-1}. The far field temperature and humidity were based on Jordan's Caribbean sounding (Gray *et al.*, 1975). In this experiment, the sea surface temperature was set to a constant 302 K and no land was present anywhere in the domain. There was neither significant environmental shear nor vertical tilt of the vortex during the evolution of the system.

Details of the simulation characterizing near-symmetric intensification (O2017): The second simulation we used was obtained from an HWRF retrospective run by Osuri *et al.* (2017). This case has also been well documented by Mohanty *et al.* (2015) and Balachandran *et al.* (2019). In summary, during the early hours of 10 October 2013, TC Phailin began rapidly intensifying in the Bay of Bengal. Over the next 24 hours, Phailin's maximum surface wind speed increased from 45 knots to 115 knots (23.15 ms^{-1} to 59.1 ms^{-1}) and the central pressure dropped from 996 hPa to 940 hPa Phailin's rapid deepening presented a major challenge to response teams, as a massive evacuation of approximately a million people had to be coordinated (Mohanty *et al.*, 2015). Balachandran *et al.* (2019) presented a numerical investigation of the processes that influenced the contrasting rapid intensity changes in TCs Phailin and Lehar (2013) over the Bay of Bengal [Figs. 1(a-d)]. Their work emphasized the differences in the environmental conditions experienced by these two TCs that occurred within a few weeks of each other and the consequent differences in the organization of vortex-scale convection that resulted in completely different evolution of the two cases. The emphasis here is on how the HWRF simulation of Phailin reproduced the *well-accepted theoretical framework of TC intensification (Ooyama, 1969).*

Details of the simulation characterizing asymmetric intensification (CG2015): The analysis used in this work to understand asymmetrical intensification in TCs was adopted from the real case study of Atlantic Hurricane Earl (2010) presented in CG2015. This run was obtained from a retrospective HWRF forecast initialized at 1800 UTC 26th August, 2010. Two phases of RI were analyzed for this simulation. The first phase of RI was centered at around 54 hours of the simulation when northerly shear was about 5 m s^{-1}. At this time, there was a significant tilt of the vortex [upper-level center displaced by about 50 km from the surface center; refer to Figs. 5(a-d) in CG2015] and the upper-level storm-relative flow[4] started advecting the warm air caused by subsidence warming in the upshear-left region towards the low level storm center [refer to Figs. 9(a&b) in CG2015]. The second phase of RI was centered at around 82 hours of the simulation when shear was about the same but when the vortex was more vertically aligned[5] and a warm core structure was better established.

We review the axisymmetric TC intensification problem in the next section using an idealized HWRF framework (GK2013). In section 3, we review the role of the PBL in the TC intensification problem using GK2013 as the basis. In section 4, we demonstrate how these idealized results are applicable to the forecast of TC Phailin (O2017). In section 5, we briefly review our recent findings on the asymmetric intensification of TCs (CG2015). In section 6, we use the tangential momentum budget for the GK2013 and CG2015 simulations to understand the role of asymmetries on the TC intensification problem. Section 7 provides concluding remarks.

2. Historical perspective of the axisymmetric TC intensification problem

A comprehensive review of the paradigms for TC intensification is provided in Montgomery and Smith (2014) and Van Sang *et al.*, (2008). We believe repeating this kind of a review may not do justice to our esteemed friends and colleagues. We therefore recommend that readers, especially students interested in pursuing research on the TC intensity problem, refer to this material. In this section, we only discuss results that form the basis for an analysis of the asymmetric TC intensification problem discussed later. Over the years, starting with the work of Charney and Eliassen (1964), there have been several simple theoretical models developed to understand the TC intensification process. In what is called the "conditional instability of the second kind" (CISK) paradigm, Charney and Eliassen (1964), for the first time, explained how the PBL "friction performs a dual role; it acts to dissipate kinetic energy, but because of the frictional convergence in the moist surface boundary layer, it acts also to supply latent heat energy to the system". In 1969, Ooyama carried out the first successful simulation of the life history of an idealized TC using three-layer, axisymmetric model that included a bulk layer for parameterizing the PBL. As articulated later, the development of the secondary circulation was central to Ooyama's (1982) "cooperative interaction" paradigm of TC intensification. In a seminal work, Emanuel (1986) provided a seamless

[4] Mean storm motion was removed for analysis

[5] Hurricane Earl never achieved absolute vertical alignment and the circulation displacement between 2 km and 8 km was about 10 km, even at the end of the 120-hour forecast.

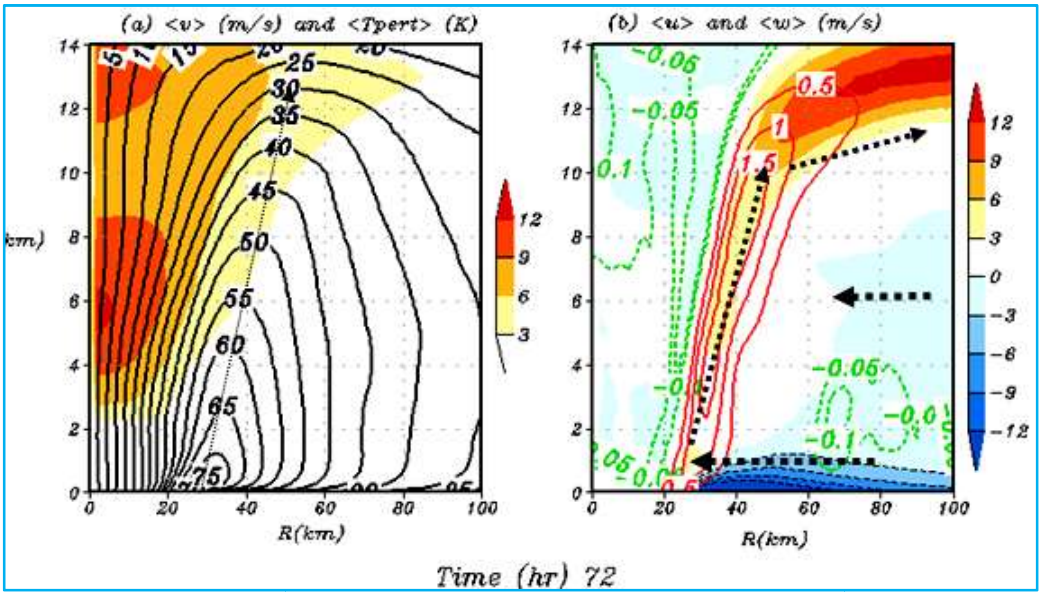

Figs. 3(a&b). Structure of an HWRF simulated idealized, symmetric, mature tropical cyclone. Radius height cross-section of the (a) primary circulation showing the azimuthally-averaged tangential wind and warm core (shaded) as measured by temperature anomaly (K) with respect to the far-field environmental temperature profile and (b) the secondary circulation that includes azimuthally-averaged inflow (shaded blue), upward (and downward) motion and the outflow (shaded red). Upward vertical velocity (ms^{-1}) is contoured in red and weak subsidence is indicated by green contours. Arrows indicate the sloping angular momentum surface and the "in-up-out" circulation

air-sea interactive framework for TC intensification. The so-called "wind-induced surface heat exchange" (WISHE) paradigm described a positive feedback between the near surface wind speed and the rate of evaporation of water from the underlying ocean (Emanuel *et al.*, 1994, section 5a; Emanuel, 2003). In addition to the assumptions of hydrostatic and gradient wind balance above the bulk PBL, where angular momentum is approximately conserved (Ooyama, 1969), air parcels were assumed to rise along the moist adiabats in Emanuel's WISHE framework [Figs. 1(a-d) in Emanuel, 1986]. Such an assumption not only greatly reduced the complexities related to parameterization of cumulus convection, but also provided an elegant way of relating the radial gradient of equivalent potential temperature above the PBL to the evaporative fluxes at the air-sea interface and, subsequently, to the maximum surface wind in the boundary layer (Fig. 6 from Montgomery and Smith, 2014). However, these axisymmetric models all assumed the middle troposphere was completely saturated and convection is symmetric around a ring. Recent three-dimensional model studies by CG2015, Leighton *et al.* (2018) and Balachandran *et al.* (2019), supported by some observational studies (e.g., Reasor, 2013 and Tao *et al.*, 2017), have illustrated the importance of asymmetries created by the environmental shear. Nevertheless, axisymmetric TC models can still be used as the basis for understanding the intensification problem.

Ooyama (1969) described TC intensification as follows: "If a weak cyclonic vortex is initially given, there will be organized convective activity in the region where the frictionally-induced inflow converges. The differential *heating due to the organized convection* introduces changes in the pressure field, which generate a *slow transverse circulation* in the free atmosphere in order to re-establish the balance between the pressure and motion fields. If the equivalent potential temperature of the boundary layer is sufficiently high for the moist convection to be unstable, the transverse circulation in the lower layer will bring in more absolute angular momentum than is lost to the sea by surface friction. Then the resulting increase of cyclonic circulation in the lower layer and the corresponding reduction of the central pressure will cause the boundary-layer inflow to increase; thus, the more intense convective activity will follow". It should also be noted that a direct consequence of solving gradient wind balance and hydrostatic balance equations leads to the thermal gradient wind relationship. The formation of a warm core is fundamental to TCs and is well supported by observations and documented in several works (e.g., Hawkins and Imbembo, 1976; Vigh and Schubert, 2009).

Figs. 3(a&b) show how the primary and secondary circulations generated by HWRF can simulate an idealized, symmetric, mature TC[6]. The azimuthally-averaged tangential wind constitutes the primary circulation [Fig. 3(a)]. The warm core shown in the figure, especially for a mature TC, can be viewed as a response to the structure of the tangential wind field. Several three-dimensional models have tried to explain warm core formation and the subsequent hydrostatic pressure drop (Chen *et al.*, 2011; Zhang and Chen, 2012; Chen and Zhang, 2013; CG2015). In a mature symmetric TC vortex, where convection is focused in the radius of the maximum wind, mass is expected to respond to tangential wind (via a thermal gradient wind relationship). Conversely, in the early intensification stages of an asymmetric vortex and the later stages of genesis where the Rossby radius of deformation may be large (e.g., Fang and Zhang, 2012), wind is expected to respond to mass. It is unclear how these basic balance arguments switch from one end of the spectra to the other in real TCs. Nevertheless, in this work we focus on the dynamical spin-up of the tangential wind.

The secondary circulation [Fig. 3(b)] is characterized by a deep layer of radial inflow about 500-m-deep from the surface and a layer of intense outflow characterizing the upper-level divergence at about 14 km height. The rising branch of the secondary circulation, depicted by red contours and located in the eyewall region, slopes radially outward and is consistent with the expected tilt in the angular momentum surfaces with height [Figs. 3(a&b) and Emanuel, 1986]. A clearly defined subsidence region in the eye of the idealized TC with more penetrative downdrafts at the eye-eyewall interface and enhanced by sublimation-evaporative cooling is also observed at about 14 km height [Fig. 3(b)], consistent with a feature noted by Zhang *et al.* (2002). The model is able to reproduce some of the observed axisymmetric features of the secondary circulation that are well documented in Marks and Houze (1987). Of specific significance to the intensification problem is the weak inflow in the middle to upper troposphere. Several axisymmetric model studies have illustrated the importance of this inflow layer to the steady evolution of a TC vortex (e.g., Yamasaki, 1977; Willoughby, 1979; Ooyama, 1982; Qin *et al*., 2018). The intensification of a TC occurs by means of cooperative interaction between the primary and secondary circulations (Ooyama, 1982). *Ooyama (1982) pointed out that the deep-layer inflow [shown by an arrow in the middle troposphere in Fig. 3(b)] is*, *in essence*, *all that is needed for intensification of cyclonic rotation (primary circulation).*

[6] To facilitate comparisons between axisymmetric model results with a fully three-dimensional model, the outputs from HWRF were transformed into a cylindrical polar coordinate system and averaged along the azimuthal direction.

It is important to note that past research using axisymmetric models focused on mature TCs rather than the evolutionary process that occurs during RI. Montgomery and Smith (2014) and Smith and Montgomery (2015) reviewed the idealized TC vortex spin-up problem in three dimensions. In contrast to a purely axisymmetric paradigm for intensification, their analysis, for the first time, recognized the presence of localized, rotating, deep-convective plumes (or vortical hot towers) that grow in both axial and radial directions in an environment of strong cyclonic vorticity within the incipient tropical storm (Hendricks *et al*., 2004). These vortical hot towers/plumes converge and stretch ambient low-level vorticity into a small-scale anomaly. The rapid spin-up of the TC vortex occurs by means of multiple mergers of the positive anomaly (Montgomery and Enagonio, 1998; Hendricks *et al.*, 2004). This process not only results in a vorticity-rich environment but also in convergence near the boundary layer that increases, producing stronger inflow. While the fully three-dimensional intensification paradigm described in Smith and Montgomery (2015) highlights the individual contributions of asymmetric, rotating, convective structures, the axisymmetric view (in an azimuthally-averaged sense) is also able to reproduce Ooyama's (1982) cooperative interaction paradigm for TC intensification [Figs. 3(a&b)] with an important additional spin-up mechanism within the PBL.

3. Role of the planetary boundary layer in tropical cyclone intensification

An extensive review of the PBL is provided in Gopalakrishnan *et al.* (2016). Starting with the study of Ekman (2005), the development of cross-isobaric flow, the secondary circulation, the subsequent PBL convergence (Charney and Eliassen, 1964) and the consequent convection in a low pressure area (Charney and Eliassen, 1964; Ooyama, 1969, 1982) have all long been recognized to play important roles in the TC intensification problem. Hence, all axisymmetric models (Ooyama, 1969; Sundqvist, 1970; Emanuel, 1986) have accounted for exchanges at the air-sea interface in their parameterization schemes. While Ooyama (1969) demonstrated the importance of both a conditionally unstable environment supporting cumulus heating and moist enthalpy fluxes at the air-sea interface as essential ingredients, Emanuel (1986) argued that "TCs are developed and maintained against dissipation entirely by self-induced anomalous fluxes of moist enthalpy from the sea surface with virtually no contribution from preexisting conditional instability". In either model, the drag coefficient (Cd) and enthalpy coefficient (Ch) were found to influence intensity changes of the simulated TC. While none of these early studies discounted the role of the PBL,

they did not take into account agradient forcing. Consequently, the inward advection of angular momentum is largely offset by frictional dissipation. However, studies by Zhang *et al.* (2001); Smith *et al.* (2009) and Gopalakrishnan *et al.* (2011, 2013) indicated that the structure of the PBL has an additional control on intensity changes in TCs. The bulk representation of the boundary and air-sea surface layer are insufficient for accurate predictions of these changes.

In Gopalakrishan *et al.* (2011), the idealized HWRF system was used to understand the impacts of model resolution on the intensification of a vertically-aligned, TC-like vortex in a shear-free environment. The study demonstrated how the model at about 3 km horizontal grid resolution produced vortex intensification consistent with the rotating convection paradigm explained in Montgomery and Smith (2014). GK2013 demonstrated that "the PBL and eyewall regions are characterized by imbalances in the gradient wind". Additionally, some imbalance prevails in the region of the outflow. Within the PBL, winds are subgradient in the outer radii but become supergradient in the eyewall region where inflow diminishes in magnitude and the convective updraft erupts. Zhang *et al.* (2001); Smith *et al.* (2009) and a series of works by Montgomery and Smith (2014) attributed the inner-core spin-up to the existence of these unbalanced flows. Specifically, the supergradient tangential winds in the region of decelerating inflow are carried upward and outward to feed into the eyewall cloud.

In GK2013, the HWRF system was again used in an idealized framework to gain a fundamental understanding of the variability in TC structure and intensity prediction that arises due to changes in vertical diffusion. Flight-level data collected by the NOAA WP3D research aircraft during eyewall penetrations of Atlantic Hurricanes Allen (1980) and Hugo (1989) at an altitude of about 450-500 m were used to improve the original medium range forecast (MRF) boundary layer parameterization scheme in the model. A reduction of the vertical eddy diffusivity to 25% of its original value resulted in a significant decrease in the height of the inflow layer. This, in turn, drastically affected the size and intensity changes in the modeled TC, making storm structure and intensity more consistent with observations (Tallapragada *et al.*, 2014). The near-surface inflow was observed to be stronger with a decrease in inflow depth. Stronger inflow not only increased the spin of the storm by enhancing the generalized Coriolis term in the equations of motion[7] for tangential velocity, but also resulted in an enhanced radial gradient of equivalent potential temperature in the boundary layer, a stronger and warmer core and, subsequently, a stronger TC. More importantly, this rapid acceleration of the inflow not only produced a stronger outflow at the top of the inflow layer, more consistent with observations, but also a smaller inner core that was less than half the size of the original and improved predictions of the radius of maximum wind (RMW). This study demonstrated that *frictional forces in the PBL may have a dual role*, *one in dissipating the angular momentum in the tangential direction* and *the other in enhancing the strength of the radial inflow in the eyewall region which can still lead to spin-up of the vortex from within the PBL.*

[7] Refer to Gopalakrishnan *et al.*, 2011 and 2013 for the governing equations

4. Symmetric intensification of tropical cyclone Phailin

TC Phailin (2013) developed in a nearly idealized environment (O2017). Warm sea surface temperatures and weak environmental shear resulted in the rapid spin-up of the vortex, closely resembling the idealized case [Figs. 3(a&b)]. Figs. 4(a-f) shows (*i*) azimuthally-averaged tangential wind (contours) and pressure perturbations as measured by anomaly (in hpa) with respect to a far-field initial environmental pressure profile, (*ii*) the secondary circulation (radial and vertical velocity; ms^{-1}) and (*iii*) azimuthally-averaged moisture perturbations as measured by anomaly (in gm/kg) with respect to a far-field environmental initial specific humidity profile and equivalent potential temperature. Figs. 4(a-c) are centered at 4 hours (prior to the initial RI phase) and Figs. 4(d-f) are centered at 13 hours (during the RI phase) of the Phailin simulation.

In an axially-averaged framework, the basic theory of intensification, discussed in section 2, is still valid during the early and later stages of RI. For a given tangential wind structure with maximum within the PBL and in approximate gradient wind balance above the PBL to start with (*i.e.*, at time = 0), heating due to persistent convection around the eyewall causes pressure changes in the column [Fig. 4(a)]. As part of the adjustment process, a secondary circulation is produced [Fig. 4(b)]. Since the radial gradient of equivalent potential temperature is high for the moist convection to be unstable [Fig. 4(c)], the transverse circulation in the lower layer will bring in more absolute angular momentum than is lost to the sea by surface friction, resulting in a strengthening of the primary circulation [Figs. 4(a&d)]. A comparison between Figs. 4(a&d) indicates that the pressure anomaly in response to persistent heating has nearly doubled by the later phase of RI [Fig. 4(d)]. This results in a stronger inflow within the boundary layer [Fig. 4(e)], accelerating radial vorticity into the eyewall region that may not be offset by diffusion or eddy fluxes. Strong moisture and equivalent potential

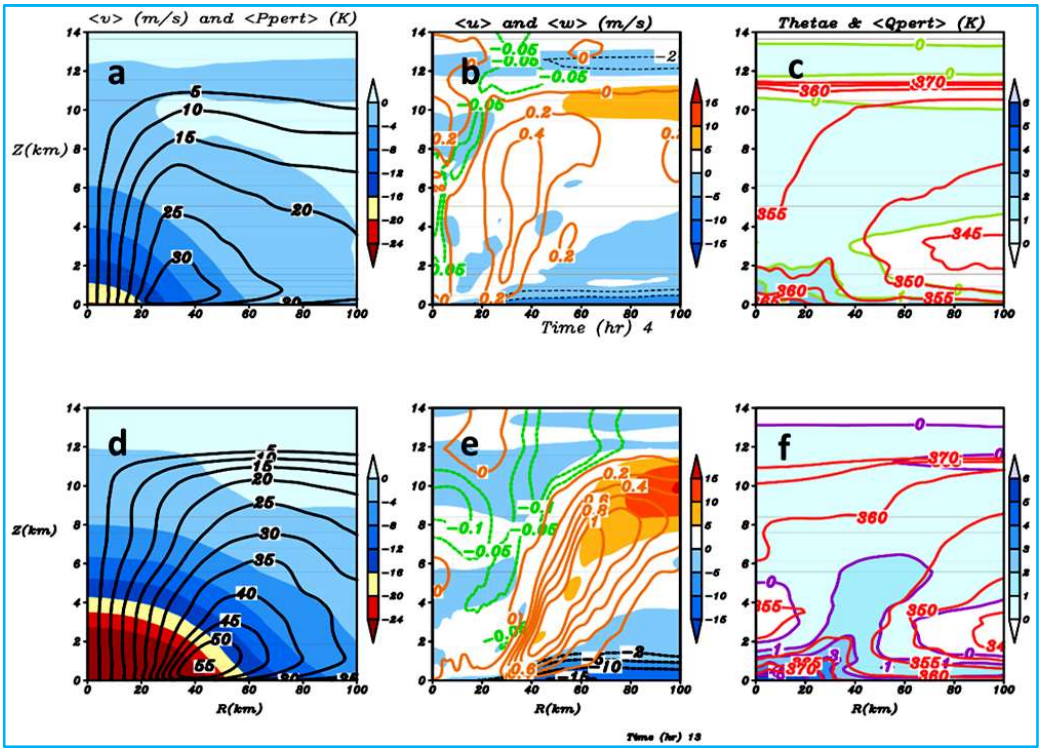

Figs. 4(a-f). (a) Azimuthally-averaged tangential wind (contours) and pressure perturbations (shaded) as measured by anomaly (in hpa) with respect to a far-field initial environmental pressure profile, (b) the secondary circulation (radial and vertical velocity; m s^{-1}), (c) azimuthally-averaged moisture perturbations as measured by anomaly (in gm/kg) with respect to a far-field initial environmental specific humidity profile (shaded) and equivalent potential temperature (contours). (a-c) are centered at 4 hours (prior to the initial RI phase) and (d-f) are centered at 13 hours (during the RI phase) of the Phailin simulation

temperature gradients between the center and outer radius are better established, indicating a mature TC circulation [Fig. 4(f)], again consistent with the theoretical framework discussed in section 2.

5. Asymmetric intensification of a tropical cyclone

Although TC Phailin (2013) rapidly intensified under near-ideal conditions, TCs are rarely axisymmetric. The asymmetric structure in the inner core of a TC may be generated by both internal dynamics and external forcing due to environmental factors such as shear and moisture. Ranging from the structure of the boundary layer (e.g., Yang *et al.*, 2007; Persing *et al.*, 2013), vortex Rossby waves (e.g., Guinn and Schubert, 1993; Montgomery and Kallenbach, 1997; Wang, 2002a, b), the eyewall (e.g., Schubert *et al.*, 1999) and mesovortices embedded in the eyewall (e.g., Black and Marks, 1991) to rainbands (e.g., Willoughby *et al.*, 1984), real TCs are characterized by a high degree of vortex-scale asymmetry. However, external forcing such as environmental shear and, consequently, the influence it has on asymmetry is much larger in scale than that generated by internal dynamics from within the vortex. Often environmental shear creates a vortex tilt[8]. Intensification usually occurs following the alignment of the vortex. Depending on the magnitude of shear, a developing TC might recover or dissipate.

In a recent study, CG2015 performed a simulation of Atlantic Hurricane Earl (2010) using the operational HWRF system. CG2015 verified the predictions of Earl against available inner-core observations and used the simulation to better understand the asymmetric RI of a TC in a sheared environment. The forecast verification illustrated that the HWRF model realistically simulated Earl's observed evolution of intensity, as well as several aspects of its inner-core structure, including convective and wind asymmetries and vortex tilt prior to and during the RI of Earl. This HWRF simulation of Earl provided a promising baseline for understanding the RI problem in three dimensions during a time period when the temporal resolution of the observations was insufficient to

[8] As measured by the circulation centers at 2 and 8 km altitude [see Figs. 5(a-d) in CG2015].

adequately study the evolution of vortex tilt and its role in the onset of RI (Rogers *et al.*, 2015). An examination of the high-resolution forecast data revealed that the tilt was large at RI onset and decreased quickly once RI commenced. Furthermore, CG2015 found that RI onset was associated with the development of upper-level warming in the eye region. A thermodynamic budget calculation showed that warming over the low-level center resulted primarily from radially-inward, storm-relative advection of subsidence-induced warm air in the upshear-left region. This advection did not occur until persistent convective bursts were concentrated in the downshear-left quadrant. It was found that the collocation of convective-scale subsidence and the broader-scale, shear-induced subsidence favored RI of the storm. When convective bursts were concentrated in the downshear-left and upshear-left quadrants, the net subsidence warming was maximized upshear and the resulting warm air advected over the low-level storm center by the upper-level, storm-relative flow. Subsequently, the surface pressure fell and RI occurred. While CG2015, for the first time, provided a thermodynamic pathway for the intensification of an asymmetric vortex, there was no consideration of dynamical processes in our earlier study (Smith and Montgomery, 2015). This raises the question: *is the well-accepted theoretical dynamical framework of TC intensification still valid for sheared storms undergoing RI?* We address this question in the following section using the Earl simulation (CG2015). The idealized simulation discussed earlier (GK2013) is used as the basis for comparison.

6. A dynamical framework for asymmetric rapid intensification

6.1. *Methodology for analysis*

To understand the influence of asymmetries on the evolution of the mean TC vortex, it is convenient to rewrite the tangential momentum equation in the cylindrical polar coordinate system (e.g., GK2013) as the sum of the mean, eddy and subgrid-scale diffusion terms (e.g., Persing *et al.*, 2013). Such a diagnostic equation is useful in understanding the vortex spin-up process, not only for an idealized and nearly upright vortex, but also for a real case like Earl where there was a significant tilt in the vortex (about 50 km) with height, at least during the initial RI process. The equation for the azimuthally-averaged wind tendency is given by:

$$\frac{\partial < v >}{\partial t} = - < u >< f + \zeta > - < w > \frac{\partial < v >}{\partial z}$$
$$- < u' \zeta' > - < w' \frac{\partial v'}{\partial z} > + < D_v > + < D_H > \qquad (1)$$

Here, the azimuthal average is denoted by < > and the departure from the azimuthal mean is denoted by the prime. The radial, tangential and vertical components of velocity in cylindrical coordinates are given by u, v and w, respectively. The vertical component of relative vorticity is given by ζ and f is the Coriolis parameter. The terms on the right-hand side of Eq. 1 are, respectively, the mean radial influx of absolute vertical vorticity, the mean vertical advection of mean tangential momentum, the eddy radial vorticity flux, the vertical eddy advection of eddy tangential momentum and the mean tendency terms due to vertical and horizontal diffusion. The residual term (not in Eq. 1), which includes the pressure gradient and numerical errors that might arise from interpolation between the model coordinate system and the cylindrical polar system used for diagnostics, was neglected. This is especially valid for the current study because the diffusion tendency terms were explicitly computed within the model. We used the outputs from the innermost (3 km) nest for our analysis and discuss the vortex spin-up mechanism in terms of Eq. 1. In all cases, the mean storm motion was removed.

6.2. *Results and discussion*

Figs. 5(a-d) shows the evolution of maximum 10-m wind speeds and the corresponding asymmetries for the idealized case and the case of Earl. Details on the evolution of these cases have already been provided in GK2013 and CG2015. Only *new findings*, mainly focused on the key questions related to asymmetries, are discussed here. The evolution of the maximum 10 m wind speed and vorticity asymmetries, calculated as the ratio of the summation of azimuthal wave numbers 1, 2, 3 and 4 magnitude over wave number 0 magnitude at 2 km(blue) and 10 km (red) height for the idealized [Fig. 5(a)] and Earl [Fig. 5(b)] cases, indicates that asymmetries are more dominant in the upper levels. In the idealized case [Fig. 5(a)], since the initial environment is cloud-free, asymmetry is small at the time of initialization. After the initial spin-up phase when the modeled microphysical processes are active, the convective asymmetry induced by the mean flow and vortex internal dynamics becomes apparent [*i.e.*, between about 6-30 hours of the simulation in Fig. 5(a)]. At around 31 hours, as the vortex intensifies, asymmetries in the upper level decrease. In the Earl case [Fig. 5(b)], the asymmetry of the initial vortex is small because of the procedure adopted in the real-time forecast (except for moisture, other microphysical variables are not cycled). However, asymmetries, especially driven by tilt, dominate the fate of the storm before RI. At 54 hours, asymmetry decreases as the vortex becomes more aligned. The RI onset is marked by a significant reduction in tilt and a rapid increase in wind speed at 57 hours [Figs. 5(b&d)], consistent with CG2015 [Figs. 5(a-d) in CG2015].

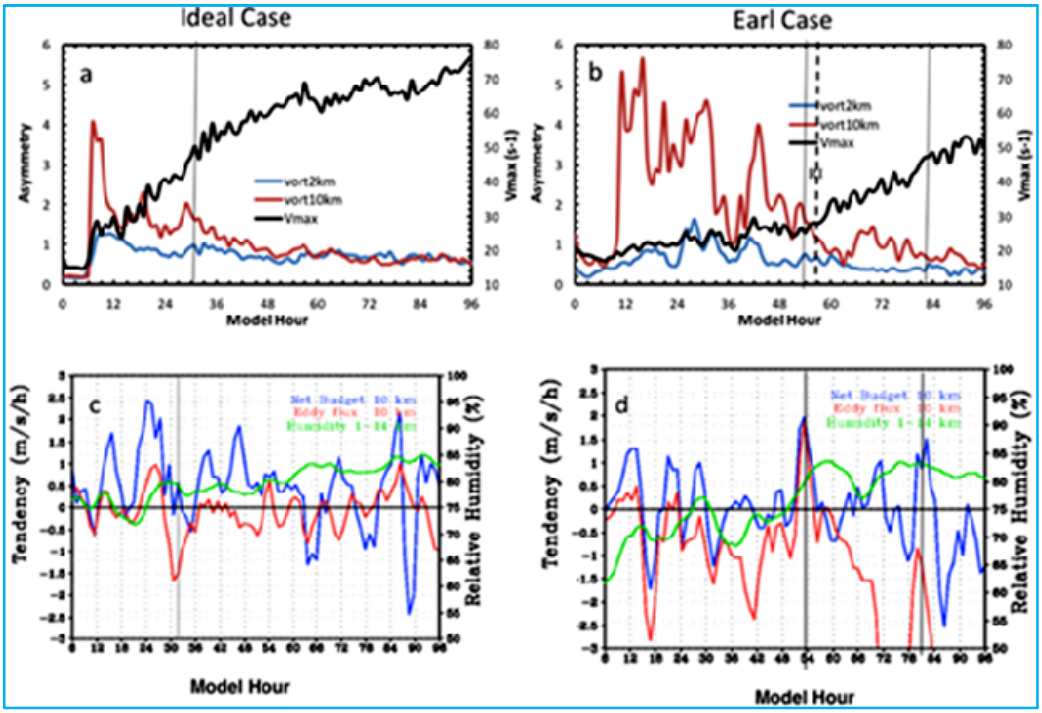

Figs. 5(a-d). Time history of evolution of the maximum 10 m wind speeds (black) and vorticity asymmetries calculated as the ratio of the summation of wave numbers 1, 2, 3 and 4 magnitude over wave number 0 magnitude at 2 km (blue) and 10 km (red) height for (a) an idealized case and (b) the Earl case. A time history of the evolution for two of the terms in the budget equation - A domain-averaged, 3-hourly time-averaged net budget (blue) and eddy radial vorticity flux (red) at 10 km and a domain-averaged, 3-hourly time-averaged relative humidity in a column between 1-10 km is provided for (c) the idealized case and (d) the Earl case. All averaging was performed within a radius of 100 km from the center of the storm. The vertical lines indicate the various periods wherein some detailed analysis was carried out

The role of the eddy radial vorticity flux in the RI problem will be discussed in detail later. Here we only show the evolution of the domain-averaged, 3-hourly time-averaged net budget (blue) and eddy radial vorticity flux (red) at 10 km, along with the domain-averaged, 3-hourly time-averaged relative humidity in a column between 1-14 km for the idealized [Fig. 5(c)] and Earl [Fig. 5(d)] cases. Montgomery and Enagonio (1998) and Hendricks *et al.* (2004) illustrated that vortex mergers may be tracked by the positive eddy radial vorticity flux. These studies also noted that the compensating effects from the mean and eddy vorticity fluxes (refer to Eq. 1) in the middle troposphere might be an indication of competing effects from hot towers (caused by upward and downward motion and the subsequent moistening and drying from individual vortical plumes). For the idealized case, there were several periods of time when vortex mergers occurred within the 100 km ring from the center [Fig. 5(c)].

As demonstrated later, the growth of the parent vortex in the case of Earl may not be attributed to individual convective-scale mergers. Nevertheless, one may notice that the total budget is dominated by a positive eddy radial vorticity flux at 54 hours [Fig. 5(d)], indicating that eddies have a positive influence on the net spin-up. It should be emphasized, however, that positive eddy radial vorticity flux alone cannot be treated as a precursor for RI. As illustrated by CG2015, the initial environment of Earl was dry; convective bursts resulted in moistening the environment. RI did not occur until the column integrated and domain-averaged relative humidity exceeded a threshold of above 75% in this case [Fig. 1(d)], thus emphasizing the importance of moisture for vortex spin-up.

Figs. 6(a-c) provides an overview of the simulations for an idealized case (GK2013), the real case of Earl (CG2015) during early RI when the vortex was tilted and at a later time when the lower and upper-level circulations of Earl were better aligned. The instantaneous structure of convection and associated asymmetries in terms of vertical velocity (shaded) and contours of vorticity fields (scaled h^{-1} for convenience) at the 10 km height are presented here. Consistent with previous studies (e.g., Hendricks *et al.*, 2004; Yang *et al.*, 2007;

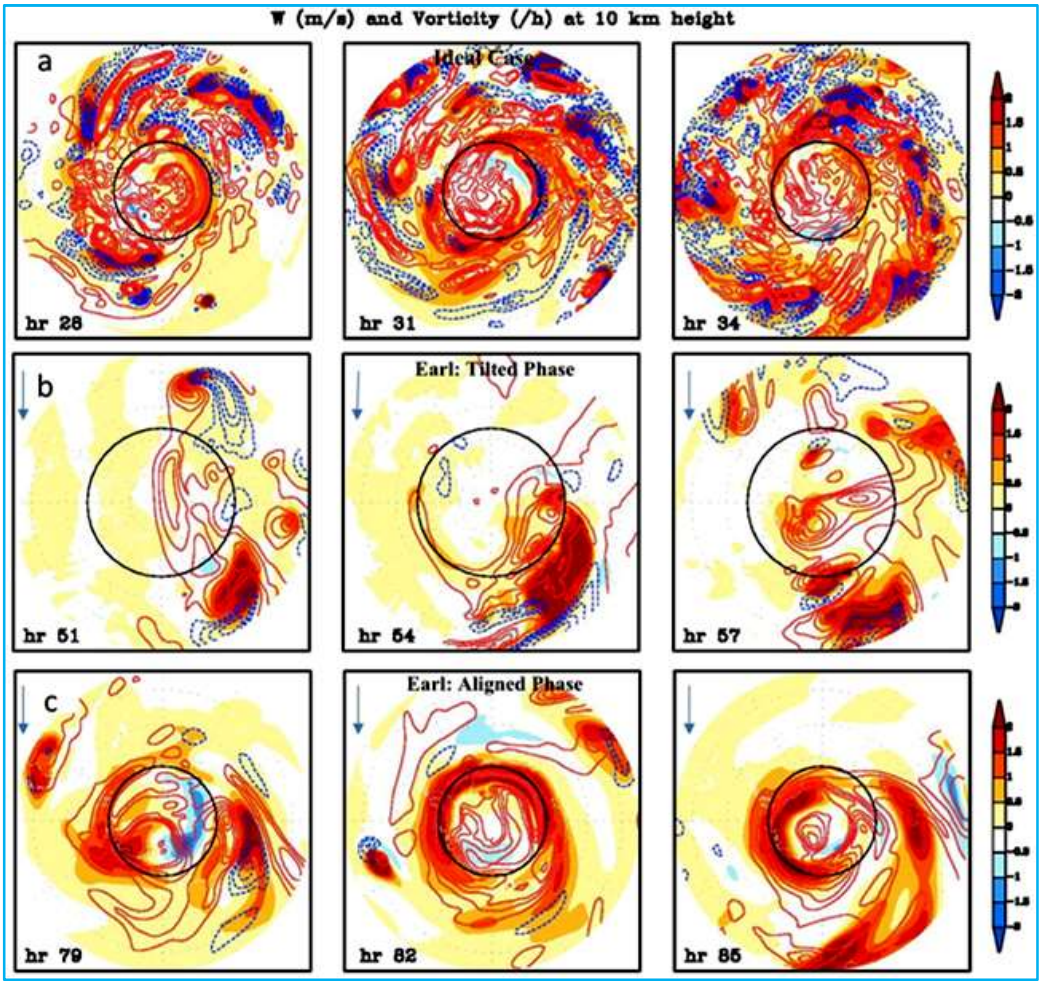

Figs. 6(a-c). Azimuthal structure of vertical velocity (in m s^{-1}, shaded) and contours of vorticity (h^{-1}) at about 10-km height during the RI of (a) an idealized vortex, (b) the Earl case when the vortex was tilted and (c) the Earl case after the vortex alignment phase. In all figures, red contours/shades denote positive values; blue contours/shades denote negative values. Contour interval is 1.0 h^{-1}. The black ring indicates the approximate radius of maximum surface wind. Each box is about 200 × 200 square kilometers. Arrow indicates the approximate direction of the shear vector (magnitude about 5.0 m s^{-1})

Nguyen *et al.*, 2008; Gopalakrishnan *et al.*, 2011; Smith and Montgomery, 2015), Fig. 6(a) shows the presence of localized, rotating, deep-convective plumes (red contours) that grow in the cyclonic, vorticity-rich environment of the incipient tropical storm in both axial and radial directions during the RI period (centered around 31 hours). By this time, within the inner core (within a 50 km radius), the initially dipolar structure of vorticity (red and blue contours) has given way to an increasingly monopolar, positive vorticity structure due to the segregation, merger and axisymmetrization process described by Nguyen *et al.* (2008).

Shear-induced asymmetries in Atlantic Hurricane Earl exhibit significant differences from that of the idealized, vertically-stacked vortex in a shear-free environment. In the early stages of RI, mesoscale convective systems, rather than vortical plumes, are organized into a highly-asymmetric pattern [Fig. 6(b)]. CG2015 demonstrated how the tilted configuration of the upper-level vortex at about 8-10 km altitude provided a more conducive environment for advection of warm air over the low-level center. Complementing these thermodynamic arguments, Fig. 6(b) shows the strengthening of vorticity with time within the radius of maximum wind. By 57 hours, although still weak and asymmetric, the inner-core region has grown richer in vorticity when compared to 51 hours (red contours within a 50 km radius). By the end of the intensification period (centered around 82 hours), despite

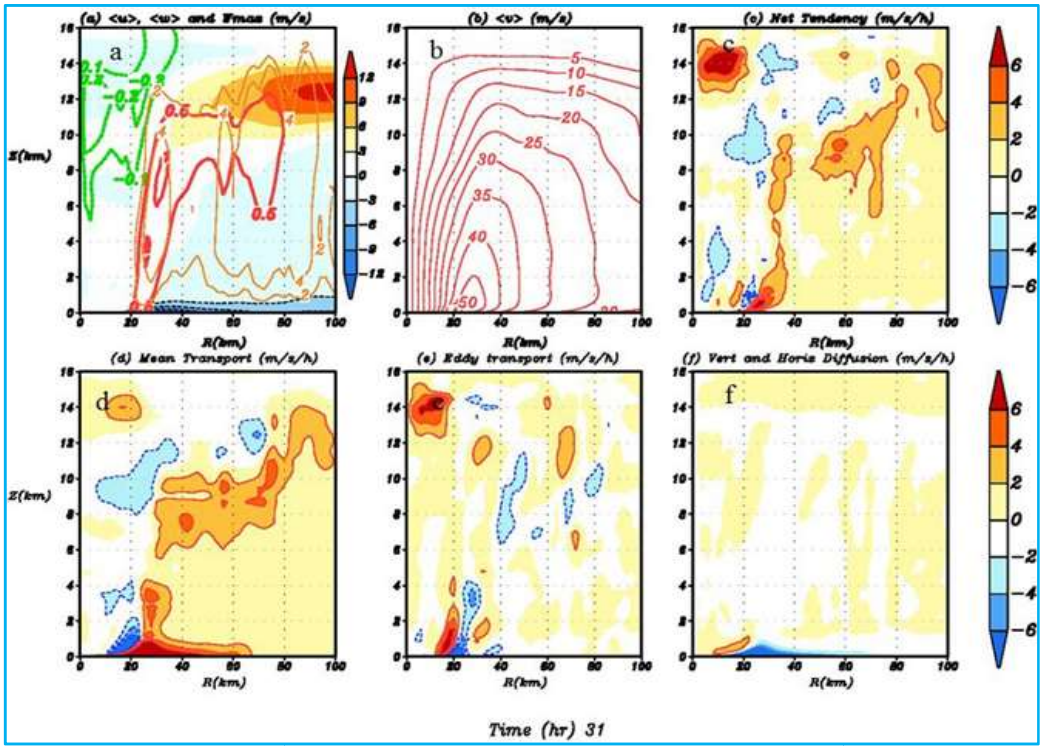

Figs. 7(a-f). Various terms in the azimuthally-averaged tangential wind tendency equation for the idealized simulation in GK2013 centered around 31 hours. In all figures, red contours/shades denote positive values; blue/green contours and blue shades denote negative values of the azimuthally-averaged, 3-hourly time-averaged, radius-height cross-section of (a) the secondary circulation (radial and vertical velocity; m s^{-1}), (b) tangential velocity (m s^{-1}), (c) net tendency after including the individual contributions from mean vertical and horizontal diffusion (m s^{-1}), (d) sum of the mean radial influx of absolute vertical vorticity and the mean vertical advection of mean tangential momentum (m s^{-1} h^{-1}), (e) sum of the eddy radial vorticity flux and the vertical eddy advection of eddy tangential momentum (m s^{-1} h^{-1}) and (f) sum of vertical and lateral diffusion terms (m s^{-1} h^{-1}). The orange contours in (a) show the maximum values of vertical velocity (m s^{-1}) around the azimuth

the shear, a well-defined eyewall and an increasingly monopolar positive vorticity structure (red contours within 50-km-radius) are established [Fig. 6(c)]. While the above section clearly illustrates the presence of asymmetries in convection and vorticity structures in the upper levels during RI [Figs. 6(a-c)], it is yet unclear how they contribute to vortex spin-up. We discuss the spin-up issue further in terms of the azimuthally-averaged wind tendency.

Figs. 7(a-f) depicts various terms in the azimuthally-averaged tangential wind tendency equation for the idealized simulation in GK2013 centered around 31 hours. In all figures, red contours/shades denote positive values, while blue/green contours and blue shades denote negative values of the azimuthally-averaged, 3-hourly time-averaged, radius - height cross section of (a) the secondary circulation (radial and vertical velocity; ms^{-1}), (b) the tangential velocity (ms^{-1}), (c) the net tendency *after including the individual contributions from mean vertical* and *horizontal diffusion* (*i.e.*, the sum of all terms on the right-hand side of Eq. 1; $ms^{-1}h^{-1}$), (d) the sum of the mean radial influx of absolute vertical vorticity and the mean vertical advection of mean tangential momentum (*i.e.*, the first two terms on the right-hand side of Eq. 1; $ms^{-1}h^{-1}$), (e) the sum of the eddy radial vorticity flux and the vertical eddy advection of eddy tangential momentum (*i.e.*, the third and fourth terms on the right-hand side of Eq. 1; $ms^{-1}h^{-1}$) and (f) the sum of the vertical and lateral diffusion terms (*i.e.*, last two terms on the right-hand side of Eq. 1; $ms^{-1}h^{-1}$). The orange contours in (a) show the contours of the maximum values of vertical velocity (ms^{-1}).

The mean structure of the HWRF modeled primary and secondary circulations for a mature idealized TC is discussed in section 2 [Figs. 3(a&b)]. During RI, radial circulation is characterized by a shallow layer of inflow about 1 km deep in the lower troposphere and a layer of intense outflow with a maximum value at about 12 km [Fig. 7(a)]. A careful analysis of Fig. 7(a) also shows rapidly swirling super gradient wind within the PBL exiting out above the layer. This outflow above the PBL

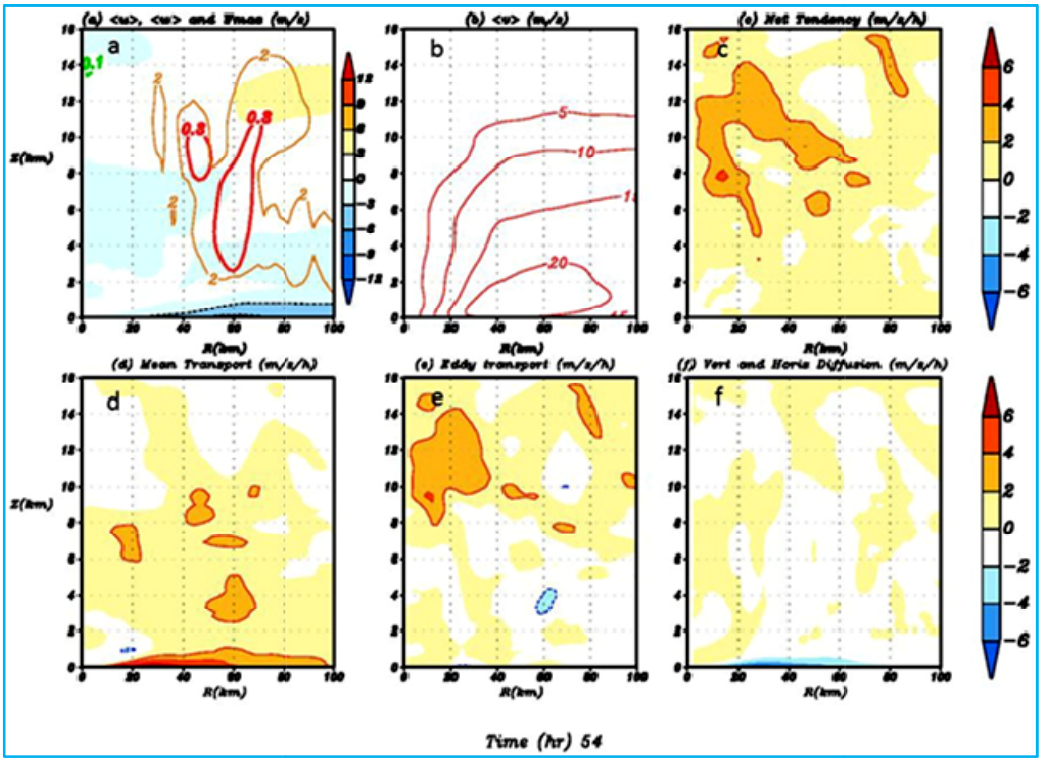

Figs. 8(a-f). Various terms in the azimuthally-averaged tangential wind tendency equation for the Earl simulation in CG2015 during RI but when there was significant vortex tilt with height. In all figures, red contours/shades denote positive values; blue/green contours and blue shades denote negative values of the azimuthally-averaged, 3-hourly time averaged, radius-height cross-section of (a) the secondary circulation (radial and vertical velocity; m s^{-1}), (b) tangential velocity (m s^{-1}), (c) net tendency after including the individual contributions from mean vertical and horizontal diffusion (m s^{-1}), (d) sum of the mean radial influx of absolute vertical vorticity and the mean vertical advection of mean tangential momentum (m s^{-1} h^{-1}), (e) sum of the eddy radial vorticity flux and the vertical eddy advection of eddy tangential momentum (m s^{-1} h^{-1}) and (f) sum of the vertical and lateral diffusion terms (m s^{-1} h^{-1}). The orange contours in (a) show the contours of the maximum values of vertical velocity (m s^{-1}) around the azimuth

strengthens to about 3 ms^{-1} at 93 hours [note shown here; Figs. 4(a-f) in GK2013]. Of significance to the intensification problem is the weak inflow in the middle to upper troposphere. The mean vertical motions [Fig. 7(a)] are characterized by a strong core updraft within the eyewall region and weak downdrafts within the developing eye. Although the mean vertical velocity is on the order of 1 ms^{-1}, extreme events of vertical motion on the order of 4 ms^{-1} are not uncommon in both the eyewall and rainband regions (Gopalakrishnan *et al*., 2011). The mean tangential wind [Fig. 7(b)] shows that the maximum value occurs within the TC boundary layer.

The mean tangential velocity budget[9] [Fig. 7(c)] during intensification for the idealized case agrees well with that presented in Persing *et al.* (2013). The budget is dominated by the mean radial influx of absolute vorticity in the hurricane boundary layer [Fig. 7(d)]. This is only partially offset by the eddy terms [Fig. 7(e)] and vertical and horizontal diffusion tendencies [Fig. 7(f)], leading to the same conclusions drawn from prior studies that spin-up of symmetric TCs occurs within the eyewall boundary layer (e.g., Zhang *et al.*, 2001; Persing *et al.*, 2013; Montgomery and Smith, 2014). There is noticeable evidence of spin-up below the axis of the outflow [Figs. 7(a&c)] and in the inner rainband region [Figs. 7(a&c)], which was also documented in Zhang *et al.* (2001) for the Atlantic Hurricane Andrew (1992) case. Likely due to strong updrafts in the rainband region [Fig. 7(a)] and the deep structure of the storm at this time [Fig. 7(b)], the vertical advection of mean tangential momentum in this region (positive contribution) is not offset by the radial outward advection of vorticity (negative contribution in the outflow region) or the eddy terms [Figs. 3(d&e)], consequently leading to a net spin-

[9] For the purpose of clarity, we have organized the terms in Eq. 1 into net, mean, eddy and diffusion terms. Conclusions discussed from these terms were drawn on the basis of a careful examination of the individual terms

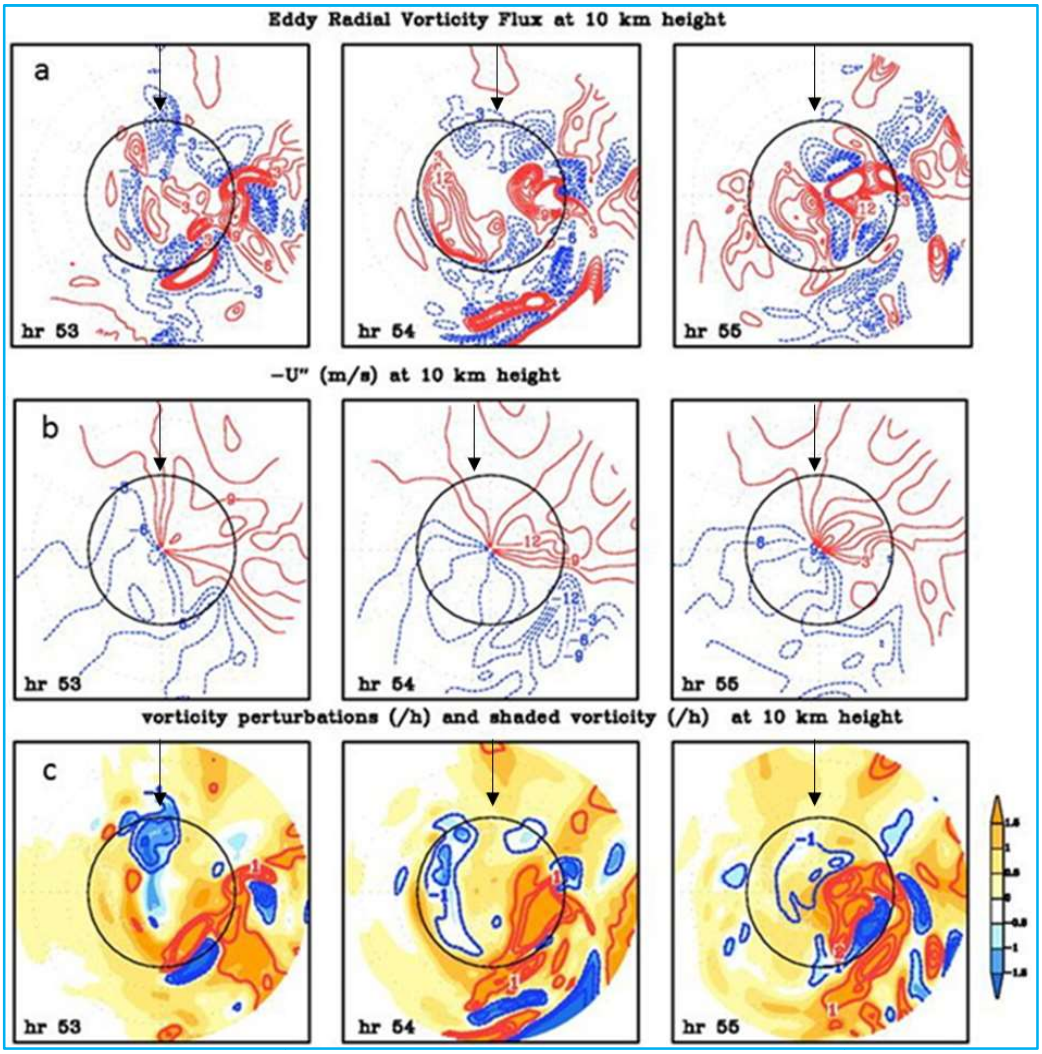

Figs. 9(a-c). Azimuthal structure of the (a) eddy radial vorticity flux (m s^{-1} h^{-1}) plotted at intervals of 3 m s^{-1} h^{-1}, (b) inflow perturbations and (c) vorticity perturbation contours superposed over vorticity (h^{-1}; shaded) at 10 km height for the Earl simulation in CG2015 during RI but when there was significant vortex tilt with height. Red contours show positive values and blue contours show negative values. The black circle indicates the 50 km radius. Arrow indicates the approximate direction of the shear vector (magnitude about 5.0 m s^{-1})

up [Fig. 7(c)]. During an RI period in this simulation, evidence of spin-down is also observed, especially on the inner edge of the eyewall region in the middle to lower troposphere [Fig. 7(c)]. As mentioned in Zhang *et al.* (2001), this spin-down is likely due to weak subsiding motion in the middle to lower troposphere [magnified in Fig. 7(a)]. As emphasized in Persing *et al.* (2013), the contributions from eddy flux terms [third and fourth terms on the right-hand side of Eq. 1; Fig. 7(e)] may not be neglected within the lower troposphere (specifically in the inner eyewall region where the flow starts to decelerate) because these terms tend to offset the spin-down by mean transport [first two terms on the right-hand side of Eq. 1; Fig. 7(d)]. Finally, it is interesting to note a small but non-negligible spin-up in the upper levels (~14-15 km height) of the eye region [Fig. 7(c)]. This positive contribution to spin-up is associated with contributions from the mean [Fig. 7(d)] and eddy [Fig. 7(e)] terms, as well as from weak inflow above the outflow layer [Fig. 7(a)]. This may be a case-dependent feature.

Figs. 8(a-f) depicts the same illustrations as in Figs. 7(a-f), except for the real-case simulation of Earl around the initial period of RI (centered around 54 hours), when there was significant vortex tilt with height. Although the mean circulation is weaker than that of the idealized vortex, mainly due to persistent shear of around 5 ms^{-1} and the tilt, the secondary and primary circulations

are well established [Figs. 8(a&b)]. However, a qualitative comparison between Figs. 8(a&b) with Figs. 7(a&b) illustrates that maximum outflow [Fig. 8(a)] is almost a third weaker than the idealized vortex. The mean tangential wind [Fig. 8(b)] is about 40% weaker than the idealized vortex. In an average sense, updrafts are weak in the eyewall region (note that the mean updraft contours were magnified to indicate the eyewall region). Nevertheless, although the azimuthal mean eyewall updrafts are relatively weak (note that mean updraft contours were magnified to indicate the eyewall region), individual updrafts are often stronger [Fig. 8(a) and Black *et al*., 1994], particularly in the downshear-left quadrant [Fig. 6(b)].

The azimuthally-averaged tangential wind budget for Earl during the early stage of RI [Fig. 8(c)] exhibits significant differences from that of the idealized, vertically-stacked vortex in a shear-free environment. It appears that the entire environment exhibits a weak background spin-up. More importantly, several idealized studies have shown that acceleration of the inflow may be an important boundary layer spin-up mechanism (e.g., GK2013; Montgomery and Smith, 2014). However, these studies [Fig. 7(a)] also reveal that strong inflow on the order of 12-20 ms^{-1} may be necessary for an accelerated spin-up of the vortex. During the early stages of RI in Earl, weak inflow [Fig. 8(a)] and, subsequently, the weak mean radial advection of vertical vorticity in the TC boundary layer [Fig. 8(d)] are nearly offset by the diffusion term[10] [Fig. 8(f)], resulting in weak contributions from the boundary layer towards the vortex spin-up process [Fig. 8(c)]. Similarly, if the mean updrafts [Fig. 8(a)] and vertical gradients in tangential winds are weak, the mean tangential advection in the eyewall region is also weak [Fig. 8(d)]. A qualitative comparison between Fig. 8(d) and Fig. 7(d) indicates the mean transport in the troposphere is much weaker in the Earl case during the early RI stage, especially in the eyewall region. Nevertheless, one of the outstanding features in this simulation is the positive contribution of eddy terms in the middle and upper troposphere to the spin-up process [Fig. 8(c)]. Clearly, as indicated in Fig. 8(e), eddy fluxes within the eyewall region and at ~8-10 km may not be neglected in the intensification of Earl. In fact, it was proved [Fig. 5(d)] that at 54 hours the mean eddy radial vertical vorticity flux is positive and the single dominant term in the mean budget calculation.

To further understand how the radial eddy flux term contributes to the growth of the parent vortex, a planar cross-section of the term (refer to Eq. 1) at 10 km altitude

[10] An analysis of individual terms showed that vertical diffusion was the dominant negative term

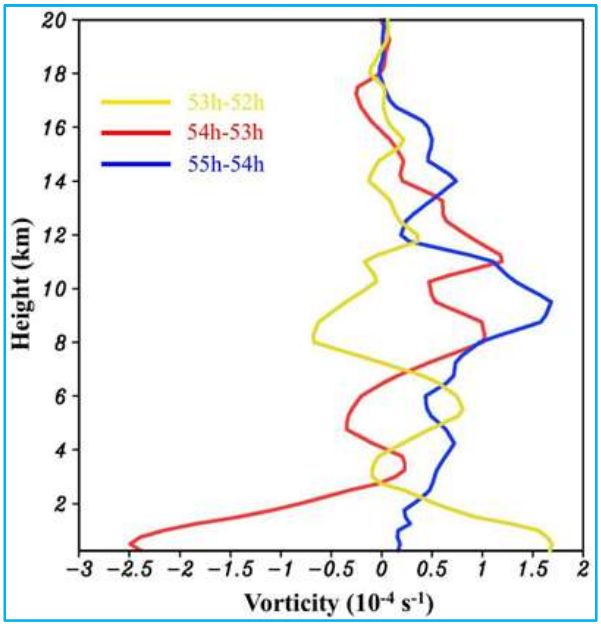

Fig. 10. Domain-averaged vorticity change between 52-53 hours, 53-54 hours and 54-55 hours; averaging was performed within a 50 km radius with respect to the lower-level center of circulation

was analyzed, centered at 54 hours when eddy contributions from the budget were positive and at a maximum. Fig. 9(a) depicts the azimuthal structure of the eddy radial vorticity flux ($ms^{-1}h^{-1}$) at 10 km height during this time. Consistent with Fig. 5(d), the positive asymmetries at 54 hours dominate within the radius of maximum winds with respect to the surface center [Fig. 9(a)]. There are two regions of strong positive values at 54 h [middle column of Fig. 9(a)], one in the west/southwest quadrant (downshear right) and the other in the eastern quadrant (downshear left). The individual contributions to the radial eddy vorticity flux from the radial wind [Fig. 9(b)] and vorticity anomaly [Fig. 9(c)] are also shown. There is a noticeable vortex scale asymmetry in the radial wind [Fig. 9(b)] due to environmental flow and vortex tilt. However, when compared to the overall change in patterns associated with the radial wind anomaly [Fig. 9(b)], the vorticity anomaly [Fig. 9(c)] appears to evolve more rapidly. Mesoscale convection in the downshear left appears to be the single largest factor that likely influences the RI of Earl. Convection in the downshear-left quadrant generates perturbation vorticity in the upper levels within a broader region of mean positive vorticity. The positive vorticity flux results from both the inward flux of positive vorticity perturbation and the outward flux of negative vorticity perturbation [Figs. 9(a-c) at 54 hours]. The net effect in the azimuthal mean is a positive contribution to the spin-up. At 55 hours, a nearly symmetric pattern of radial eddy

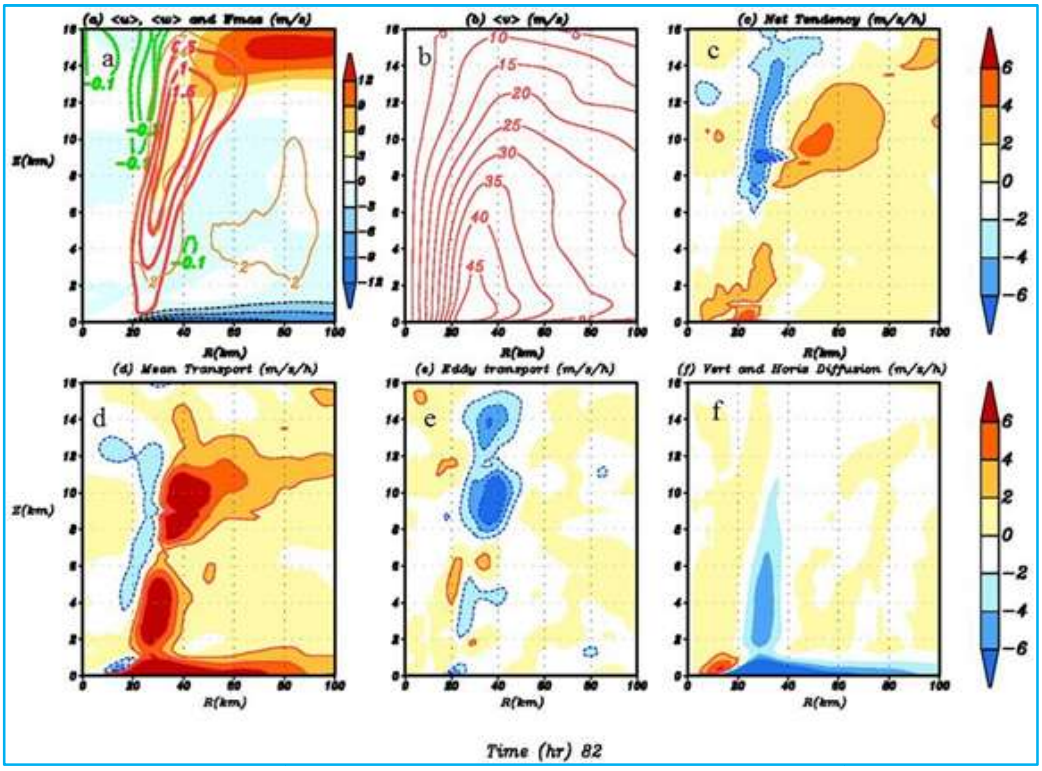

Figs. 11(a-f). Various terms in the azimuthally-averaged tangential wind tendency equation for the Earl simulation during RI but at 82 hours. In all figures, red contours/shades denote positive values; blue/green contours and blue shades denote negative values of the azimuthally-averaged, 3-hourly time averaged, radius–height cross section of (a) the secondary circulation (radial and vertical velocity; m s^{-1}), (b) tangential velocity (m s^{-1}), (c) net tendency after including the individual contributions from mean vertical and horizontal diffusion (m s^{-1}), (d) sum of the mean radial influx of absolute vertical vorticity and the mean vertical advection of mean tangential momentum (m s^{-1} h^{-1}), (e) sum of the eddy radial vorticity flux and the vertical eddy advection of eddy tangential momentum (m s^{-1} h^{-1}) and (f) sum of the vertical and lateral diffusion terms (m s^{-1} h^{-1}). The orange contours in (a) show the contours of the maximum values of vertical velocity (m s^{-1}) around the azimuth

vorticity flux [Fig. 9(a)] surrounds the center,indicating that vorticity anomalies have merged to create a stronger mean vortex wherein the upper and lower level circulations are better aligned. This process of vortex alignment is also supported by the sudden decay of asymmetries after this time [Fig. 5(c)].

In the case of Earl, the persistent shear and tilt phase locks convection in the downshear-left quadrant. As seen in Fig. 6(b), as these mesoscale convective complexes move from the downshear-left quadrant to the upshear-left quadrant and inward towards the lower level circulation center, collocated positive vorticity and its perturbations increase inward and within the 50 km ring until the mean vorticity in the ring increases. A plot of changes in domain-averaged (mean) vorticity within the 50 km ring (Fig. 10) clearly shows that the middle to upper level vorticity increases consistently from 53-55 hours. The mesoscale convection in the downshear-left quadrant [Figs. 6(b) and Fig. 5(c)], especially between 54-55 hours, sets up a vorticity-rich environment that includes a larger part of the middle to upper troposphere [Fig. 6(a-c)] for the subsequent intensification process. In summary, despite shear and a lack of symmetric convection, persistent convective bursts in the downshear quadrant that propagate slowly to the upshear direction and inward are sufficient to align the vortex. The alignment results in faster spin-up of the nearly vertically-stacked vortex [Fig. 8(c)].

Figs. 11(a-f) depicts various terms in the azimuthally-averaged tangential wind tendency equation for the real-case simulation of Earl at the end of the RI period (centered around 82 hours). Environmental shear is about 5 ms^{-1}, but the vortex is vertically better aligned Consistent with the established and nearly symmetric eyewall in Fig. 6(c), both the primary and secondary circulations [Figs. 11(a&b)] are strong and well developed at this time. As in the case of the idealized simulation, the

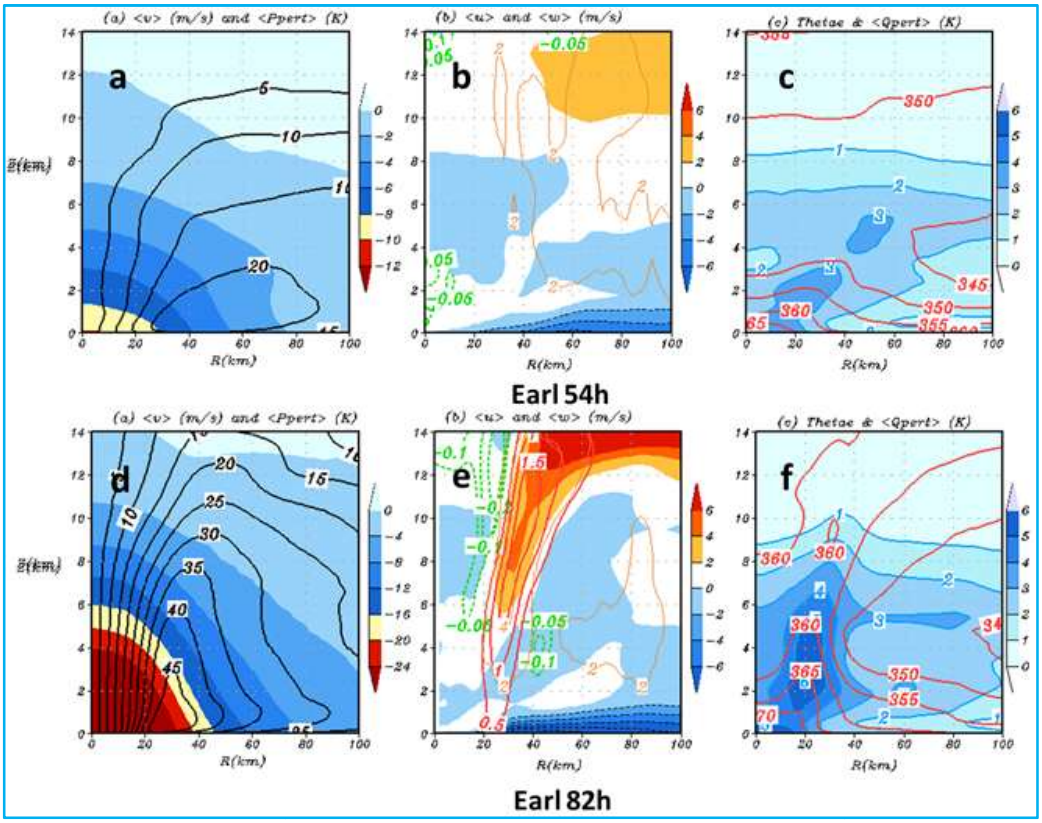

Figs. 12(a-f). (a) Azimuthally-averaged tangential wind (contours) and pressure perturbations (shaded) as measured by anomaly (in hpa) with respect to a far-field initial environmental pressure profile, (b) the secondary circulation (radial and vertical velocity; ms^{-1}) and (c) azimuthally-averaged moisture perturbations as measured by anomaly (in gm/kg) with respect to a far-field initial environmental specific humidity profile (shaded) and equivalent potential temperature (contours). (a-c) are centered at 54 hours (initial RI phase) and (d-f) are centered at 82 hours (later RI phase) of the Earl simulation. The orange contours in (b) and (e) show the maximum values of vertical velocity (ms^{-1}) around the azimuth

budget is dominated by a mean radial influx of absolute vertical vorticity in the hurricane boundary layer [Figs. 11(c&d)] that is only partially offset by the eddy terms and diffusion tendencies within the PBL [Figs. 11(e&f)]. As a consequence, spin-up within the boundary layer and eyewall is observed [Fig. 11(c)]. Again, consistent with the idealized simulation, there is significant spin-up in the eyewall and below the axis of the outflow, as well as in the inner rainband region [Fig. 11(c)]. Likely due to strong updrafts [Fig. 11(a)] and the deep structure of the storm at this time [Fig. 11(b)], the vertical advection of mean tangential momentum in this region (positive contribution; Eq. 1) is not offset by the radial outward advection of vorticity (negative contribution in the outflow region; Eq. 1). However, due to persistent shear, the eddy terms in the eyewall region [Fig. 11(e)] appear to play a significant role in counteracting, at least partially, the spin-up associated with mean vertical advection in this region [Fig. 11(d)]. Evidence of spin down, especially along the inner edge of the eyewall region in the middle to upper troposphere, is also observed [Fig. 11(c)]. This is very likely associated with the noticeable subsidence present during this time [Fig. 11(a)].

Previous studies have suggested that flow asymmetries generally play a negative role in storm intensification (e.g., Yang *et al*., 2007; Bryan *et al*., 2010). Leighton *et al.* (2018) used an ensemble simulation from Atlantic Hurricane Edouard (2014) and computed the momentum budgets used here to isolate the effect of the eddy vorticity flux in an intensifying and weakening ensemble member. The study found that the positive radial eddy vorticity flux for RI members contributed significantly to spinning up the tangential wind in the middle and upper levels and reduced vortex tilt. The negative eddy vorticity flux for non-intensifying members spun down the tangential wind in the middle and upper levels and did not help the vortex become vertically aligned.

Finally, we address the question posed in the introduction: *Is the well-accepted theoretical framework of TC intensification still valid for sheared storms undergoing RI?* Figs. 12(a-f) shows (a) the azimuthally-averaged tangential wind (contours) and pressure anomaly (in hPa) with respect to a far-field environmental reference profile of pressure at an initial time, (b) the secondary circulation (radial and vertical velocity; m s^{-1}) and (c) the moisture anomaly (in gm/kg) with respect to a far-field environmental reference profile of specific humidity at an initial time. Figs. 12(a-c) are centered at 54 hours, while Figs. 12(d-f) are centered at 82 hours of the Earl simulation. Although a fully three-dimensional model is required to understand the real TC intensification problem, when viewed from an axially-averaged framework, the basic theory of intensification discussed in section 2 is still valid during the early and later stages of RI. During the early stages of intensification, a well-defined eyewall is absent [Figs. 12(b)]. Nevertheless, heating due to persistent convection in the downshear-left quadrant [Figs. 6(b)] is sufficient to create mean pressure perturbations [Figs. 12(a)] and sustain a well-defined inflow channel within the PBL [Figs. 12(b)] for advecting moisture to the eyewall region [Figs. 12(c)]. A weak inflow above the PBL, consistent with Ooyama (1969), is also observed [Figs. 12(b)] in response to heating due to the mesoscale convection above the PBL. However, as depicted by the mean equivalent temperature profiles [Figs. 12(c)], asymmetric heating is not efficient enough to produce a strong warm core structure. Nevertheless, about a day later, despite persistent shear, convection is better organized and more symmetrical around the eyewall region [Figs. 6(c)]. Consistent with the more symmetric structure, the eyewall convection [Figs. 12(e)] is stronger. A comparison between Figs. 12(a&d) indicates that the pressure anomaly nearly doubles in response to the more symmetrical heating. This results in stronger inflow within the boundary layer, accelerating radial vorticity into the eyewall region that may not be offset by diffusion or eddy fluxes [Figs. 11(c-f)]. The mean tangential wind also more than doubles [Figs. 12(a&d)]. Strong moisture and equivalent potential temperature gradients between the center and outer radius are well established, indicating a mature TC circulation, again consistent with the theoretical framework discussed in section 2.

7. Summary and concluding remarks

Accurate TC intensity prediction is of importance to forecasting because early guidance of the strength of a TC and its rainfall distribution has the potential to save lives, as well as reduce property damages. At the same time, the topic is also of research interest. Supported with observations and starting with the work of Reihl in the 1950s, some checkered advancements have been made in understanding TCs using theoretical and simple axisymmetric models. However, until recently, forecasting intensity changes in TCs has been a challenge, partly because this multiscale problem requires both high-resolution, non-hydrostatic, three-dimensional models to not only resolve the inner core structure of a TC but to also accurately resolve the interactions between the TC vortex and its environment. Initializing forecast models at the highest resolution has also been a challenge. So theoretical research has always led forecast research until recently. To address the intensity forecast problem, NOAA created HFIP in 2009. The high-resolution HWRF system was created under this program. The HWRF system is now paving the way in removing the initial roadblocks associated with predicting intensity changes, the dynamical prediction of which was nearly non-existent before 2009 (Gopalakrishnan and coauthors, 2019). In an effort to bridge this state-of-the-art forecasting system with the existing theoretical framework, we used the HWRF system to first verify whether the model could reproduce the basic paradigm of intensification set forth by those theoretical models. Since most of our understanding until recently has been driven by axisymmetric models, we used an idealized simulation in a shear-free environment and a forecast of an ideally behaved TC over the Bay of Bengal (*i.e.*, TC Phailin, 2013) to illustrate how the axially-averaged results from the HWRF forecast system might be able to explain the basic intensification process.

TCs are rarely axisymmetric. Environmental shear can create large asymmetries in the TC scale circulation. We sought to address the following questions here: *How do TCs rapidly intensify in a sheared environment? What is the role of asymmetries on TC intensification? Is the well-accepted theoretical framework of TC intensification still valid for sheared storms undergoing RI?* We used a high-resolution retrospective run from Atlantic Hurricane Earl (2010) to better understand the role of shear-induced asymmetries on the RI of TCs. Based on this work and other parallel research, our findings show that eddy radial vorticity fluxes play a significant role in controlling TC intensity changes in sheared storms. In the case of Earl, despite persistent environmental shear and a lack of symmetric convection, a positive eddy vorticity flux in the middle and upper troposphere created by mesoscale convective systems had a profound influence on accelerating the TC spin-up process.

RI does not occur until persistent convective bursts and the collocated vertical vorticity are concentrated in the downshear-left quadrant and at about 50 km from the surface center, followed by propagation of these convective complexes to the upshear direction. When convective bursts reach the upshear-left quadrant, a nearly

symmetric pattern of eddy radial vorticity flux surrounds the center, indicating that vorticity anomalies have merged to create a stronger mean vortex wherein the upper and lower level circulations are better aligned. This process is different from that of an idealized vortex. An idealized vortex intensifies in a shear-free environment where individual vortical hot plumes converge and stretch ambient low-level vorticity into a small-scale anomaly and multiple mergers of these plumes lead to a single stronger vortex. More importantly, while for the idealized case the major spin-up of the vortex occurs in the TC boundary layer and eyewall region, the spin-up in the case of Earl appears to be top-down[11] during the early stages of intensification. Nevertheless, evidence of stronger spin-up is observed in the boundary layer after the initial RI phase. Although a fully three-dimensional model is required to understand the real TC intensification problem, when viewed from an axially-averaged framework, the basic axisymmetric theory of intensification is still valid in all cases.

The influence of eddies on intensity changes in TCs is a topic of ongoing research and may be of relevance for providing forecast guidance-on-guidance, especially when using ensemble products. Recently, Leighton *et al.* (2018) used experimental forecasts from the operational HWRF-based ensemble prediction system for Atlantic Hurricane Edouard (2014) and analyzed the differences in both the RI inner-core structure and large-scale environment between RI and non-intensifying (NI) ensemble members. A budget analysis of tangential momentum revealed that the radial eddy vorticity flux contributed positively to the spin-up of tangential winds in the middle to upper levels and reduced vortex tilt in the RI member. In contrast, the negative eddy vorticity flux for the NI member spun down the tangential winds in the middle to upper levels and did not vertically align the vortex. According to Leighton *et al.* (2018), "This difference suggests that positive radial eddy vorticity flux is a key term that contributes to intensity change in a sheared environment by spinning up the tangential winds in the middle to upper levels and reducing tilt. As the vortex becomes more symmetric and vertically aligned, the radial advection of mean vorticity becomes the dominant term that contributes to the continuing intensification of the RI member".

Another ensemble study (Hazelton, personal communication) that used a high-resolution (3 km) nested version of the Finite Volume Cube Sphere (FV3)-Global Forecast System (Hazelton *et al.*, 2018a,b), which is part of the evolving Unified Forecast System being developed by NOAA, was used to gain some fundamental understanding of RI in Atlantic Hurricane Michael (2018). The hurricane is a classic example of a TC that intensified into a strong Category-5 TC over the Gulf of Mexico despite more than 20 knots of large-scale shear for much of its lifetime. Again, while the RI members showed positive eddy vorticity fluxes increasing with time, perhaps a sign of vortex resilience to shear, the NI members showed no such trend.

Although until recently the research community mainly focused on the dynamics of a storm's inner core (*i.e.*, within about 200 km of the storm center), much of the real-time intensity change problem involves external influences on the TC circulation. The current effort is expected to bridge the gaps in our understanding of how different the structure and, subsequently, the intensification of a three-dimensional TC vortex can be due to shear, yet be viewed from an axially-averaged framework where the basic axisymmetric theory of intensification is still valid. The current investigation did not focus on the effect of dry air. Nevertheless, using the idealized framework of HWRF (Gopalakrishnan *et al.*, 2011), our investigation showed that, in the absence of shear, dry air causes a delay in RI. Further, Balachandran *et al.* (2019) presented a numerical investigation of the processes that influenced the contrasting RI changes in TCs Phailin and Lehar (2013) over the Bay of Bengal using the HWRF system. While both TCs initially underwent RI, Lehar dissipated due to shear. Balachandran *et al.* (2019) found the cause-and-effect mechanism: middle level dry air intrusion and venting were a follow-up of the spin-down of the upper-level TC circulation due to shear. Nevertheless, a full investigation of the effect of dry air on an evolving vortex such as Earl (2010) or Edouard (2014) may be required. However, this may not be easy to isolate because shear is usually associated with dry air in the upshear quadrant and not the other way around.

Beyond the environmental shear (and dry air) discussed here, structure and intensity changes in TCs are affected by a number of other asymmetries that can arise from within the vortex. Vortex Rossby waves (Montgomery and Kallenbach, 1997) formed in the presence of large vorticity gradients are found to be responsible for the formation of spiral rainbands (e.g., Willoughby). Similarly, polygonal features and mesovortices and the associated vorticity mixing may have significant impact on the evolution of TC structure (Schubert *et al.*, 1999; Kossin *et al.*, 2000; Kossin and Schubert, 2001; Rozoff *et al.*, 2006). While it is unclear at this time if such asymmetries may be a cause or an effect of intense convection and related intensity changes, vortex-scale asymmetries associated with eyewall replacement cycles in TCs are known to drive TC

[11] The word "top-down" is a misnomer because convergence has its origin in the boundary layer. Nevertheless, it is used here in the context of spin-up in the PBL versus the middle and upper troposphere.

intensity changes (e.g., Zhu *et al.*, 2015 and Tyner *et al.*, 2018 are two recent works using the HWRF system). Although eyewall replacement cycles are known to impact intensity forecasts, there is a general lack in both understanding and predicting these cycles in TCs.

Air-sea interactions in TCs, which are no less complex (Gopalakrishnan *et al.*, 2016) involve a spectrum of processes that could potentially control TC intensity change. While it is well known that an increase in SSTs should fuel a stronger hurricane because of the increase in both latent and sensible heat fluxes and ocean coupled models are essential to improve intensity predictions, it appears that both waves, as well as sea spray, may have a huge impact on the intensification process. Several pioneering works using the GFDL model by Isaac Ginis and his group members (Moon *et al.*, 2007, 2008; Bender *et al.*, 2007; Fan *et al.*, 2009a,b) are starting to demonstrate the importance of ocean waves under hurricane conditions. Air-sea (momentum, heat, moisture) fluxes and turbulent mixing above/below the air-sea interface in tropical cyclones are greatly modified by surface waves. Size and asymmetries in the structure of TCs might have a huge influence on ocean waves, which in turn affect the roughness (*i.e.*, Cd) and subsequently, the momentum transfer between the atmosphere and the ocean surface. While the rough, yet, non-breaking waves may act as a sink of angular momentum in the PBL, the breaking waves may counter those effects by the creation of sea spray that may have some significant influence on the enthalpy fluxes (both sensible as well as latent) and on the TC intensification process. The life cycle of an individual spray drop is complex (Andreas and Emanuel, 2001). In most of the cases, all the factors discussed above interact non-linearly during the lifetime of a TC. No wonder cycle to cycle variability and storm to storm variability is not uncommon and makes the TC forecasting problem a challenging one!

Acknowledgements

The authors acknowledge NOAA's Hurricane Forecast Improvement Program (HFIP) and the Implementation Arrangement between NOAA and the Ministry of Earth Sciences, India. Thanks are due to Dr.K.J.Ramesh for his support of the HWRF system at the India Meteorological Department. Most part of the review material in this manuscript originated from a lecture series provided by the first author at the Indian Institute of Technology, Bhubaneswar under the Global Initiative Academic Network (GIAN) program. Thanks are due to Profs. Michael Montgomery and Roger Smith and several Hurricane Research Division scientists for initiating some very useful debates related to the dynamics of Tropical Cyclone vortex in the presence of shear. Drs. Michael Fischer, Xiaomin Chen andrew Hazelton, George Alvey and Lew Gramer from the Hurricane Research Division of NOAA reviewed the manuscript. Their help is greatly acknowledged. Thanks are due to Ms. Gail Derr for offering excellent editorial support.

The contents and views expressed in this research paper are the views of the authors and do not necessarily reflect the views of the organizations they belong to.

References

Andreas, E. L. and Emanuel, K. A., 2001, "Effects of sea spray on tropical cyclone intensity", *Journal of the Atmospheric Sciences*, **58**, 3741-3751.

Atlas, R., Tallapragada, V. and Gopalakrishnan, S., 2015, "Advances in tropical cyclone intensity forecasts", *Marine Technology Society Journal*, **49**, 149-160.

Bao, J. W., Gopalakrishnan, S. G., Michelson, S. A., Marks, F. D. and Montgomery, M. T., 2012, "Impact of physics representations in the HWRFX on simulated hurricane structure and pressure-wind relationships", *Monthly Weather Review*, **140**, 3278-3299.

Bender, M. A., Ginis, I., Tuleya, R., Thomas, B. and Marchok, T., 2007, "The operational GFDL coupled hurricane-ocean prediction system and a summary of its performance", *Monthly Weather Review*, **135**, 3965-3989.

Bhalachandran, S., Nadimpalli, R., Osuri, K. K., Marks Jr., F. D., Gopalakrishnan, S., Subramanian, S., Mohanty, U. C. and Niyogi, D., 2019, "On the processes influencing rapid intensity changes of tropical cyclones over the Bay of Bengal", *Scientific Reports*, **9**, 3382.

Black, P., 1983, "Tropical storm structure revealed by stereoscopic photographs from Skylab", *Advances in Space Research*, **2**, 115-124.

Black, R. A., Bluestein, H. B. and Black, M. L., 1994, "Unusually strong vertical motions in a Caribbean hurricane", *Monthly Weather Review*, **122**, 2722-2739.

Bryan, G. H., Rotunno, R. and Chen, Y., 2010, "The effects of turbulence on hurricane intensity", 29th Conference on Hurricanes and Tropical Meteorology, Tucson, AZ, *Amer. Meteor. Soc.*, 8C.7, https://ams.confex.com/ams/29Hurricanes/techprogram/paper_167282.htm.

Byers, H., 1944, "Atmospheric Turbulence and the Wind Structure near the Surface of the Earth", Ch. XXIV. in General Meteorology, McGraw-Hill Book Co., Inc., New York.

Charney, J. G. and Eliassen, A., 1964, "On the growth of the hurricane depression", *Journal of the Atmospheric Sciences*, **21**, 68-75.

Chen, H. and Gopalakrishnan, S. G., 2015, "A Study on the Asymmetric Rapid Intensification of Hurricane Earl (2010) Using the HWRF System", *Journal of the Atmospheric Sciences*, **72**, 531-550.

Chen, H. and Zhang, D. L., 2013, "On the Rapid Intensification of Hurricane Wilma (2005). Part II: Convective Bursts and the Upper-Level Warm Core", *Journal of the Atmospheric Sciences*, **70**, 146-162.

Chen, H., Zhang, D. L., Carton, J. and Atlas, R., 2011, "On the Rapid Intensification of Hurricane Wilma (2005). Part I: Model Prediction and Structural Changes", *Weather and Forecasting*, **26**, 885-901.

Chen, X., Wang, Y., Fang, J. and Xue, M., 2018, "A numerical study on rapid intensification of Typhoon Vicente (2012) in the South China Sea. Part II: Roles of inner-core processes", *J. Atmos. Sci.*, **75**, 235-255, doi:10.1175/JAS-D-17-0129.1.

Demaria, M. and Kaplan, J., 1994, "A statistical hurricane intensity prediction scheme (SHIPS) for the Atlantic basin", *Weather and Forecasting*, **9**, 209-220.

DeMaria, M., 1996, "The effect of vertical shear on tropical cyclone intensity change", *Journal of the Atmospheric Sciences*, **53**, 2076-2087.

Eastin, M. D., Gray, W. M. and Black, P. G., 2005a, "Buoyancy of convective vertical motions in the inner core of intense hurricanes. Part I: General statistics", *Monthly Weather Review*, **133**, 188-208.

Eastin, M. D., Gray, W. M. and Black, P. G., 2005b, "Buoyancy of convective vertical motions in the inner core of intense hurricanes. Part II: Case studies", *Monthly Weather Review*, **133**, 209-227.

Ekman, V. W., 1905, "On the influence of the earth's rotation on ocean-currents".

Emanuel, K. A., 1986, "An air sea interaction theory for tropical cyclones Part I: Steady-state maintenance", *Journal of the Atmospheric Sciences*, **43**, 585-604.

Emanuel, K. A., Neelin, J. D. and Bretherton, C. S., 1994, "On large-scale circulations in convecting atmospheres", *Quarterly Journal of the Royal Meteorological Society*, **120**, 1111-1143.

Emanuel, K., 2003, "A similarity hypothesis for air-sea exchange at extreme wind speeds", *Journal of the Atmospheric Sciences*, **60**, 1420-1428.

Fan, Y. L., Ginis, I. and Hara, T., 2009a, "The effect of wind-wave-current interaction on air-sea momentum fluxes and ocean response in tropical cyclones", *Journal of Physical Oceanography*, **39**, 1019-1034.

Fan, Y. L., Ginis, I., Hara, T., Wright, C. W. and Walsh, E. J., 2009b, "Numerical simulations and observations of surface wave fields under an extreme tropical cyclone", *Journal of Physical Oceanography*, **39**, 2097-2116.

Fang, J. and Zhang, F. Q., 2012, "Effect of Beta Shear on Simulated Tropical Cyclones", *Monthly Weather Review*, **140**, 3327-3346.

Fischer, M. S., Tang, B. H. and Corbosiero, K. L., 2017, "Assessing the influence of upper-tropospheric troughs on tropical cyclone intensification rates after genesis", *Mon. Wea. Rev.*, **145**, 1295-1313, https://doi.org/10.1175/MWR-D-16-0275.1.

Frank, W. M. and Ritchie, E. A., 2001, "Effects of vertical wind shear on the intensity and structure of numerically simulated hurricanes", *Monthly Weather Review*, **129**, 2249-2269.

Gopalakrishnan, S. G., Goldenberg, S., Quirino, T., Zhang, Marks Jr., X. F., Yeh, K. S., Atlas, R. and Tallapragada, V., 2012, "Toward Improving High-Resolution Numerical Hurricane Forecasting: Influence of Model Horizontal Grid Resolution, Initialization and Physics", *Weather and Forecasting*, **27**, 647-666.

Gopalakrishnan, S. G., Marks, F., Zhang, X. J., Bao, J. W., Yeh, K. S. and Atlas, R., 2011, "The Experimental HWRF System: A Study on the Influence of Horizontal Resolution on the Structure and Intensity Changes in Tropical Cyclones Using an Idealized Framework", *Monthly Weather Review*, **139**, 1762-1784.

Gopalakrishnan, S. G., Marks, F., Zing, J. A., Zhang, X., Bao, J. W. and Tallapragada, V., 2013, "A study of the impacts of vertical diffusion on the structure and intensity of the tropical cyclones using the high-resolution HWRF system", *Journal of the Atmospheric Sciences*, **70**, 524-541.

Gopalakrishnan, S. G., Srinavas, C. V. and Bhatia, K., 2016, "The hurricane boundary layer", *Advanced Numerical Modeling* and *Data Assimilation Techniques for Tropical Cyclone Predictions*, Mohanty, U. C. and Gopalakrishnan, S. G. (eds.), Springer Netherlands, 589-626.

Gopalakrishnan, S. G., Toepfer, F., Koch, Dorothy, Upadhayay, S., DeMaria, M., Marks, F., Rappaport, E. N., Mehra, Avichal, Tallapragada, V., Alaka Jr., G., Bender, M., Bernardet, L., Cione, J., Biswas, M., Brennan, M., Cangialosi, J., Doyle, J., Franklin, J. L., Gramer, L., Halliwell, G., Hazelton, A., Hilderbrand, J. S., Kalina, E., Kim, H. S., Kucera, P., Kurkowski, N., Lett, N., Liu, Bin, McCaslin, P., Mifflin, E., Morin, M., Moskaitis, J., Musgrave, K., Nance, L., Newman, K., Onderlinde, M., Penny, A., Simon, A., Sippel, J., Tolman, H., Torn, R., Wang, X., Whitaker, J., Winterbottom, H., Zelinsky, D. A., Zhang, F., Zhang, X., Zhang, Z. and Zhu, Lin, 2019, "2018 HFIP R&D Activities Summary: Recent Results and Operational Implementation, *HFIP Technical Report*, (http://www.hfip.org/documents/HFIP_AnnualReport_FY2018.pdf)

Gray, W. M., 1968, "Role of cumulus vertical momentum transport in dynamics of hurricane eye-wall region", *Bulletin of the American Meteorological Society*, **49**, 1026-1045.

Gray, W. M., Ruprecht, E. and Phelps, R., 1975, "Relative humidity in tropical weather systems", *Monthly Weather Review*, **103**, 685-690.

Guinn, T. A. and Schubert, W. H., 1993, "Hurricane spiral bands", *Journal of the Atmospheric Sciences*, **50**, 3380-3403.

Hack, J. J. and Schubert, W. H., 1986, "Nonlinear response of atmospheric vortices to heating by organized cumulus convection", *Journal of the Atmospheric Sciences*, **43**, 1559-1573.

Halliwell, G. R., Gopalakrishnan, S., Marks, F. and Willey, D., 2015, "Idealized Study of Ocean Impacts on Tropical Cyclone Intensity Forecasts", *Monthly Weather Review*, **143**, 1142-1165.

Hawkins, H. F. and Imbembo, S. M., 1976, "Structure of a small, intense hurricane - Inez 1966", *Monthly Weather Review*, **104**, 418-442.

Hazelton, A. T., Bender, M., Morin, M., Harris, L. and Lin, S. J., 2018a, "2017 Atlantic hurricane forecasts from a high-resolution version of the GFDL fvGFS model: Evaluation of track, intensity and structure", *Weather and Forecasting*, **33**, 1317-1337.

Hazelton, A. T., Harris, L. and Lin, S. J., 2018b, "Evaluation of tropical cyclone structure forecasts in a high-resolution version of the multiscale GFDL fvGFS model", *Weather and Forecasting*, **33**, 419-442.

Hendricks, E. A., Montgomery, M. T. and Davis, C. A., 2004, "The role of "vortical" hot towers in the formation of tropical cyclone Diana (1984)", *Journal of the Atmospheric Sciences*, **61**, 1209-1232.

Kaplan, J. and DeMaria, M., 2003, "Large-scale characteristics of rapidly intensifying tropical cyclones in the North Atlantic basin", *Weather* and *Forecasting*, **18**, 1093-1108.

Kossin, J. P. and Schubert, W. H., 2001, "Mesovortices, polygonal flow patterns and rapid pressure falls in hurricane-like vortices", *Journal of the Atmospheric Sciences*, **58**, 2196-2209.

Kossin, J. P., Schubert, W. H. and Montgomery, M. T., 2000, "Unstable interactions between a hurricane's primary eyewall and a secondary ring of enhanced vorticity", *Journal of the Atmospheric Sciences*, **57**, 3893-3917.

Leighton, H., Gopalakrishnan, S., Zhang, J. A., Rogers, R. F., Zhang, Z. and Tallapragada, V., 2018, "Azimuthal distribution of deep convection, environmental factors and tropical cyclone rapid intensification: A perspective from HWRF ensemble forecasts of Hurricane Edouard (2014)", *Journal of the Atmospheric Sciences*, **75**, 275-295.

Marks, F. D. and Houze, R. A., 1987, "Inner core structure of Hurricane Alicia from airborne Doppler RADAR observations", *Journal of the Atmospheric Sciences*, **44**, 1296-1317.

Marks, F. D., Black, P. G., Montgomery, M. T. and Burpee, R. W., 2008, "Structure of the eye and eyewall of Hurricane Hugo (1989)", *Monthly Weather Review*, **136**, 1237-1259.

Merrill, R. T., 1988, "Environmental-influences on hurricane intensification", *Journal of the Atmospheric Sciences*, **45**, 1678-1687.

Mohanty, U. C., Osuri, Krishna K., Tallapragada, Vijay, Marks, Frank D., Pattanayak, Sujata, Mohapatra, M., Gopalakrishnan, S. G. and Niyogi, Dev, 2015, "A Great Escape from the Bay of Bengal 'Super Sapphire-Phailin' Tropical Cyclone - A case of improved weather forecast and societal response for disaster mitigation", *Earth Interactions*, **19**, 1-11.

Molinari, J. and Vollaro, D., 2010, "Rapid Intensification of a Sheared Tropical Storm", *Monthly Weather Review*, **138**, 3869-3885.

Molinari, J., Dodge, P., Vollaro, D., Corbosiero K. L. and Marks, F., 2006, "Mesoscale aspects of the downshear reformation of a tropical cyclone", *Journal of the Atmospheric Sciences*, **63**, 341-354.

Montgomery, M. T. and Enagonio, J., 1998, "Tropical cyclogenesis via convectively forced vortex rossby waves in a three-dimensional quasigeostrophic model", *Journal of the Atmospheric Sciences*, **55**, 3176-3207.

Montgomery, M. T. and Kallenbach, R. J., 1997, "A theory for vortex Rossby-waves and its application to spiral bands and intensity changes in hurricanes", *Quarterly Journal of the Royal Meteorological Society*, **123**, 435-465.

Montgomery, M. T. and Smith, R. K., 2014, "Paradigms for tropical cyclone intensification", *Australian Meteorological* and *Oceanographic Journal*, **64**, 37-66.

Moon, I. J., Ginis, I. and Hara, T., 2008, "Impact of the reduced drag coefficient on ocean wave modeling under hurricane conditions", *Monthly Weather Review*, **136**, 1217-1223.

Moon, I. J., Ginis, I., Hara, T. and Thomas, B., 2007, "A physics-based parameterization of air-sea momentum flux at high wind speeds and its impact on hurricane intensity predictions", *Monthly Weather Review*, **135**, 2869-2878.

Nguyen, S., Smith, R. and Montgomery, M., 2008, "Tropical-cyclone intensification and predictability in three dimensions", *Q. J. R. Meteorol. Soc.*, **134**, 563-582.

Ooyama, K. V., 1982, "Conceptual evolution of the theory and modeling of the tropical cyclone", *Journal of the Meteorological Society of Japan*, **60**, 369-380.

Ooyama, K., 1969, "Numerical simulation of life cycle of tropical cyclones", *Journal of the Atmospheric Sciences*, **26**, 1, 3-40.

Osuri, K. K., Nadimpalli, R., Mohanty, U. C. and Niyogi, D., 2017, "Prediction of rapid intensification of tropical cyclone Phailin over the Bay of Bengal using the HWRF modelling system", *Quarterly Journal of the Royal Meteorological Society*, **143**, 678-690.

Persing, J., Montgomery, M. T., McWilliams, J. C. and Smith, R. K., 2013, "Asymmetric and axisymmetric dynamics of tropical cyclones", *Atmospheric Chemistry and Physics*, **13**, 12299-12341.

Qin, N., Zhang, D. L., Miller, W. and Kieu, C. Q., 2018, "On the rapid intensification of Hurricane Wilma (2005). Part IV: Inner-core dynamics during the steady RMW stage", *Q. J. Roy. Meteor. Soc.*, **144**, 717, 2508-2523, doi:10.1002/qj.3339.

Reasor, P. D., Eastin, M. D. and Gamache, J. F., 2009, "Rapidly intensifying Hurricane Guillermo (1997). Part I: Low-wave number structure and evolution", *Monthly Weather Review*, **137**, 603-631.

Reasor, P. D., Rogers, R. and Lorsolo, S., 2013, "Environmental flow impacts on tropical cyclone structure diagnosed from airborne doppler radar composites", *Monthly Weather Review*, **141**, 2949-2969, doi: 10.1175/MWR-D-12-00334.1.

Riehl, H., 1954, "Rainfall and vorticity advection", *Journal of Meteorology*, **11**, 425-427.

Riemer, M., Montgomery, M. T. and Nicholls, M. E., 2010, "A new paradigm for intensity modification of tropical cyclones: Thermodynamic impact of vertical wind shear on the inflow layer", *Atmospheric Chemistry and Physics*, **10**, 3163-3188.

Rogers, R. F., Reasor, P. D. and Zhang, J. A., 2015, "Multiscale structure and evolution of Hurricane Earl (2010) during rapid intensification", *Monthly Weather Review*, **143**, 536-562.

Rozoff, C. M., Schubert, W. H., McNoldy, B. D. and Kossin, J. P., 2006, "Rapid filamentation zones in intense tropical cyclones", *Journal of the Atmospheric Sciences*, **63**, 325-340.

Schubert, W. H. and Hack, J. J., 1982, "Inertial stability and tropical cyclone development", *Journal of the Atmospheric Sciences*, **39**, 1687-1697.

Schubert, W. H., Montgomery, M. T., Taft, R. K., Guinn, T. A., Fulton, S. R., Kossin, J. P. and Edwards, J. P., 1999, "Polygonal eyewalls, asymmetric eye contraction and potential vorticity mixing in hurricanes", *Journal of the Atmospheric Sciences*, **56**, 1197-1223.

Shay, L. K., Goni, G. J. and Black, P. G., 2000, "Effects of a warm oceanic feature on Hurricane Opal", *Monthly Weather Review*, **128**, 1366-1383.

Smith, R. K. and Montgomery, M. T., 2015, "Toward clarity on understanding tropical cyclone intensification", *Journal of the Atmospheric Sciences*, **72**, 3020-3031.

Smith, R. K., Montgomery, M. T. and Sang, N. Van, 2009, "Tropical cyclone spin-up revisited", *Quarterly Journal of the Royal Meteorological Society*, **135**, 1321-1335.

Sundqvist, H., 1970, "Numerical simulation of development of tropical cyclones with a 10-level model Part II", *Tellus*, **22**, 5, 504-510.

Tallapragada, V., Kieu, C., Kwon, Y., Trahan, S., Liu, Q. F., Zhang, Z. and Kwon, I. H., 2014, "Evaluation of Storm Structure from the Operational HWRF during 2012 Implementation", *Monthly Weather Review*, **142**, 4308-4325.

Tallapragada, V., Kieua, C., Trahana, S., Liua, Q., Wanga, W., Zhanga, Z., Tonga, M., Zhang, B., Zhua, L. and Strahl, B., 2015, "Forecasting Tropical Cyclones in the Western North Pacific Basin Using the NCEP Operational HWRF: Real-Time Implementation in 2012", *Weather* and *Forecasting*, **30**, 1355-1373.

Tang, B. and Emanuel, K., 2010, "Midlevel ventilation's constraint on tropical cyclone intensity", *Journal of the Atmospheric Sciences*, **67**, 1817-1830.

Tang, B. and Emanuel, K., 2012, "Sensitivity of tropical cyclone intensity to ventilation in an axisymmetric model", *J. Atmos. Sci.*, **69**, 2394-2413.

Tao, C., Jiang, H. and Zawislak, J., 2017, "The relative importance of stratiform and convective rainfall in rapidly intensifying tropical cyclones", *Mon. Wea. Rev.*, **145**, 795-809, doi:10.1175/ MWR-D-16-0316.1.

Tyner, B., Zhu, P., Zhang, J. A., Gopalakrishnan, S., Marks, F. and Tallapragada, V., 2018, "A top-down pathway to secondary eyewall formation in simulated tropical cyclones", *Journal of Geophysical Research Atmospheres*, **123**,174-197.

Van Sang, N., Smith, R. K. and Montgomery, M. T., 2008, "Tropical-cyclone intensification and predictability in three dimensions", *Quarterly Journal of the Royal Meteorological Society*, **134**, 563-582.

Vigh, J. L. and Schubert, W. H., 2009, "Rapid development of the tropical cyclone warm core", *Journal of the Atmospheric Sciences*, **66**, 3335-3350.

Wang, Y. Q., 1995, "An inverse balance equation in sigma-coordinates for model initialization", *Monthly Weather Review*, **123**, 482-488.

Wang, Y., 2002a, "Vortex Rossby waves in a numerically simulated tropical cyclone. Part II: The role in tropical cyclone structure and intensity changes", *Journal of the Atmospheric Sciences*, **59**, 1239-1262.

Wang, Y., 2002b, "Vortex Rossby waves in a numerically simulated tropical cyclone. Part I: Overall structure, potential vorticity and kinetic energy budgets", *Journal of the Atmospheric Sciences*, **59**, 1213-1238.

Willoughby, H. E., 1979, "Forced secondary circulations in hurricanes", *Journal of Geophysical Research-Oceans* and *Atmospheres*, **84**, 3173-3183.

Willoughby, H. E., 1990a, "Gradient balance in tropical cyclones", *Journal of the Atmospheric Sciences*, **47**, 265-274.

Willoughby, H. E., 1990b, "Temporal changes of the primary circulation in tropical cyclones", *Journal of the Atmospheric Sciences*, **47**, 242-264.

Willoughby, H. E., Clos, J. A. and Shoreibah, M. G., 1982, "Concentric eye walls, secondary wind maxima and the evolution of the hurricane vortex", *Journal of the Atmospheric Sciences*, **39**, 395-411.

Willoughby, H. E., Marks, F. D. and Feinberg, R. J., 1984, "Stationary and moving convective bands in hurricanes", *Journal of the Atmospheric Sciences*, **41**, 3189-3211.

Yamasaki, M., 1977, "A preliminary experiment of the tropical cyclone without parameterizing the effects of cumulus convection", *Journal of the Meteorological Society of Japan. Ser. II*, **55**, 11-31.

Yang, B., Wang, Y. Q. and Wang, B., 2007, "The effect of internally generated inner-core asymmetries on tropical cyclone potential intensity", *Journal of the Atmospheric Sciences*, **64**, 1165-1188.

Zhang, D. L. and Chen, H., 2012, "Importance of the upper-level warm core in the rapid intensification of a tropical cyclone", *Geophysical Research Letters*, **39**, 2, L02806.

Zhang, D. L., Liu, Y. B. and Yau, M. K., 2001, "A multiscale numerical study of Hurricane Andrew (1992). Part IV: Unbalanced flows", *Monthly Weather Review*, **129**, 92-107.

Zhang, D. L., Liu, Y. B. and Yau, M. K., 2002, "A multiscale numerical study of Hurricane Andrew (1992). Part V: Inner-core thermodynamics", *Monthly Weather Review*, **130**, 2745-2763.

Zhang, X. J., Gopalakrishnan, S. G., Trahan, S., Quirino, T. S., Liud, Q., Zhang, Z., Alaka, G. and Tallapragadad, V., 2016, "Representing Multiple Scales in the Hurricane Weather Research and Forecasting Modeling System: Design of Multiple Sets of Movable Multilevel Nesting and the Basin-Scale HWRF Forecast Application", *Weather and Forecasting*, **31**, 2019-2034.

Zhu, P., Zhu, Z., Gopalakrishnan, S., Black, R. A., Marks, F. D., Tallapragada, V. S., Zhang, J. A., Zhang, X. and Gao, C., 2015, "Impact of subgrid-scale processes on eyewall replacement cycle of tropical cyclones in HWRF system", *Geophysical Research Letters*, **42**, 10027-10036.